

VARIATIONAL BAYES' METHOD FOR FUNCTIONS WITH APPLICATIONS TO SOME INVERSE PROBLEMS

JUNXIONG JIA, QIAN ZHAO, DEYU MENG*, AND ZONGBEN XU

ABSTRACT. Bayesian approach as a useful tool for quantifying uncertainties has been widely used for solving inverse problems of partial differential equations (PDEs). One of the key difficulties for employing Bayesian approach is how to extract information from the posterior probability measure. Variational Bayes' method (VBM) is firstly and broadly studied in the field of machine learning, which has the ability to extract posterior information approximately by using much lower computational resources compared with the sampling type method. In this paper, we generalize the usual finite-dimensional VBM to infinite-dimensional space, which makes the usage of VBM for inverse problems of PDEs rigorously. General infinite-dimensional mean-field approximate theory has been established, and has been applied to abstract linear inverse problems with Gaussian and Laplace noise assumptions. Finally, some numerical examples are given which illustrate the effectiveness of the proposed approach.

1. INTRODUCTION

Motivated by significant applications in medical imaging, seismic explorations and so on, the field of inverse problems has undergone an enormous development over the last few decades. For handling an inverse problem, we usually meet ill-posed in the sense that the solution lacks of stability or even uniqueness [24, 38]. Regularization approach, including Tikhonov regularization and Total-Variation regularization, is one of the most popular approaches to alleviate the ill-posed natural of inverse problems. Using regularization method, an estimated function will be provided, however, there is no uncertainty analysis about the estimated solution.

Bayesian inverse approach provides a flexible framework for inverse problems by transforming it into statistical inference problems, which provides uncertainty analysis for the solution of inverse problems. Inverse problems usually accompanied with a forward operator originated from some partial differential equations (PDEs), which brings difficulties to the direct use of finite-dimensional Bayes' formula. There are two strategies can be employed:

- (1) Discretize-then-Bayesian: The PDEs are first discretized to approximate the original problem in some finite-dimensional space and the reduced approximate problem is then solved using Bayes' method;

2010 *Mathematics Subject Classification.* 65L09, 49N45, 62F15.

Key words and phrases. Variational Bayes' method, Inverse problems, Inverse source problem, Uncertainty quantification.

- (2) Bayesian-then-discretize: The Bayes' formula and algorithms are constructed on infinite-dimensional space firstly. And once the infinite-dimensional algorithm is posed, some finite-dimensional approximation is carried out.

The first strategy makes all the Bayesian inference method developed in the statistical literatures available [28]. However, due to the original problems are defined on infinite-dimensional space, problems such as inconvergence and dimensional dependence emerged for using this strategy [29]. By employing the second strategy, discretization-invariant property are naturally holds since the Bayes' formula and algorithms are properly defined on some separable Banach space [16, 37]. In the following, we confine ourselves to the second strategy, that is postpone the discretization to the final step.

One of the most important issue for employing Bayes' inverse method is that how to extract information from the posterior probability measure. For current studies, there are two major approaches: point estimates and sampling method. For point estimates, maximum a posteriori (MAP) estimate is commonly utilized, which intuitively equivalent to solve an optimization problem. Only recently, some rigorous analysis are provided [1, 8, 15, 17, 21] for this intuitive equivalence relation. In some situations [25, 38], MAP estimates are more desirable and computationally feasible than the entire posterior distribution. However, point estimates can not provide uncertainty quantification and usually recognized as an incomplete Bayes' method.

For extracting all the information encoded in the posterior distribution, sampling methods such as Markov chain Monte Carlo (MCMC) are often employed. In 2013, Cotter et al [13] propose MCMC method for functions, which ensures that the speed of convergence of the algorithms is robust under mesh refinement. Then, a lot of dimension-independent MCMC type algorithms are proposed [14, 19]. Although MCMC is a high-efficient sampling method, its computational cost (at least 10^5 samples are commonly needed) is still unacceptable for many applications, e.g., full waveform inversion.

Here, we aim to provide a variational method that can perform uncertainty analysis and, in the mean time, with a comparative computational cost as for computing MAP estimates. For the finite-dimensional problems, such types of methods named as variational Bayes' methods (VBM) are firstly and broadly investigated in the field of machine learning [6, 33, 40, 41]. For its applications to inverse problems, Jin et al [27, 26] employed VBM to investigate a hierarchical formulation of finite-dimensional inverse problems when the noise distributed according to Gaussian or centered-t distribution. Then, Guhua et al [20] generalize the method further to the case when the noise distributed according to skew-t error distribution. Recently, finite-dimensional VBM has been applied to study porous media flows in heterogeneous stochastic media [39].

All of the investigations mentioned above are based on finite-dimensional VBM, hence, only the first strategy mentioned before can be employed to solve inverse problems. To the best of our knowledge, there are only two relevant works about VBM under infinite-dimensional setting. Specifically, when the approximate probability measures are restricted to be Gaussian, Pinski et al [34, 35] employ a calculus of variations viewpoint to study the properties of Gaussian approximate sequences with the measure of fit chosen to be Kullback-Leibler (KL) divergence. Relying on Robbins-Monro algorithm, a novel algorithm has been constructed to

attain the approximate Gaussian measure. Until now, there seems no corresponding investigations beyond the Gaussian approximate measure assumption. However, various types of approximate probability measures have been frequently used for training deep neural networks and solving finite-dimensional inverse problems [27, 26]. Hence, for applications in inverse problems concerned with PDEs, it is crucial to construct VBM with approximate measures beyond Gaussian on infinite-dimensional space.

In the following, we focus on the classical mean-field approximation employed for finite-dimensional case, which originally stems from the theory of statistical mechanics for treating many-body systems. Inspired by the finite-dimensional theory, we construct a general infinite-dimensional mean-field approximate based VBM, which allows non-Gaussian approximate probability measures to be employed. Then, two examples are given to illustrate the flexibility of the proposed approach. In summary, the contributions of our work are as follows:

- By introducing a reference probability measure and using calculus of variations, we establish a general mean-field approximate based VBM on separable Hilbert space, which provides a flexible framework for introducing techniques developed on finite-dimensional space to infinite-dimensional space.
- We apply the proposed general theory to a general linear inverse problem with Gaussian and Laplace noise assumptions respectively. Through detailed calculations, we construct iterative algorithms for functions. To the best of our knowledge, VBM with Laplace noise assumption has not been employed for solving inverse problems even restricted to finite-dimensional space.
- We solve inverse source problems of Helmholtz equations with multi-frequency data by the proposed VBM with Gaussian and Laplace noise assumptions. The algorithms not only provide a point estimate but also give the standard deviations of the numerical solutions. For such a high computational cost problem, it seems hardly to employ sampling algorithms such as MCMC, however, the VBM can provides reasonable results.

The outline of this paper is as follows. In Section 2, we construct the general infinite-dimensional VBM based on the mean-field approximate assumption. In Section 3, under the hierarchical formulation, we apply the general theory to an abstract linear inverse problem with Gaussian and Laplace noise assumptions. In Section 4, concrete numerical examples are given to illustrate the effectiveness of the proposed approach. In Section 5, we give a summarization and some future research problems. Finally, we provide all of the proofs in appendix.

2. GENERAL THEORY ON INFINITE-DIMENSIONAL SPACE

In Subsection 2.1 we present some basic background theory and prove some basic results concerned with the existence of minimizers for finite product probability measures. In Subsection 2.2 we provide a variational Bayes' approach on infinite-dimensional space, which will be applied to some general linear inverse problems in Section 3. In order to show the main ideas fluently, all of the proof details are postponed to the Appendix.

2.1. Existence theory. In this subsection, we recall some general facts about Kullback-Leibler (KL) approximation from the viewpoint of calculus of variations,

and then provide some new theorems for product of probability measures that form the basis of our investigation. Let \mathcal{H} be a separable Banach space endowed with its Borel sigma algebra $\mathcal{B}(\mathcal{H})$, and denote by $\mathcal{M}(\mathcal{H})$ the set of Borel probability measures on \mathcal{H} .

For inverse problems, we usually need to find a probability measure μ on \mathcal{H} , named as the posterior probability measure, specified by its density with respect to a prior probability measure μ_0 . We assume the Bayesian formula on Banach space defined by

$$(2.1) \quad \frac{d\mu}{d\mu_0}(x) = \frac{1}{Z_\mu} \exp(-\Phi(x)),$$

where $\Phi(x) : \mathcal{H} \rightarrow \mathbb{R}$ is a continuous function, and that $\exp(-\Phi(x))$ is integrable with respect to μ_0 . The constant Z_μ is chosen to ensure that μ is indeed a probability measure.

Let $\mathcal{A} \subset \mathcal{M}(\mathcal{H})$ be a set of “simpler” measures that can be efficiently calculated, then our aim is to find the closest element ν to μ with respect to Kullback-Leibler (KL) divergence from the subset \mathcal{A} . For any $\nu \in \mathcal{M}(\mathcal{H})$ that is absolutely continuous with respect to μ , the KL divergence is defined as follow

$$(2.2) \quad D_{\text{KL}}(\nu||\mu) = \int_{\mathcal{H}} \log\left(\frac{d\nu}{d\mu}(x)\right) \frac{d\nu}{d\mu}(x) \mu(dx) = \mathbb{E}^\mu \left[\log\left(\frac{d\nu}{d\mu}(x)\right) \frac{d\nu}{d\mu}(x) \right],$$

where the convention $0 \log 0 = 0$ has been used. If ν is not absolutely continuous with respect to μ , then the KL divergence is defined as $+\infty$. With this definition, the main aims of this paper can be formulated as for investigating the following minimization problem

$$(2.3) \quad \underset{\nu \in \mathcal{A}}{\operatorname{argmin}} D_{\text{KL}}(\nu||\mu).$$

Concerning the above general minimization problem (2.3), there are some studies [18, 35] from the perspective of calculus of variations. In this subsection, we follow the line of these investigations. For the reader’s convenience, we list the following proposition which is proved in [35].

Proposition 2.1. Let \mathcal{A} be closed with respect to weak convergence. Then, for given $\mu \in \mathcal{M}(\mathcal{H})$, assume that there exists $\nu \in \mathcal{A}$ such that $D_{\text{KL}}(\nu||\mu) < \infty$. It follows that there exists a minimizer $\nu \in \mathcal{A}$ solving

$$\underset{\nu \in \mathcal{A}}{\operatorname{argmin}} D_{\text{KL}}(\nu||\mu).$$

As stated in the introduction, we aim to construct mean-field approximation which usually takes a factorized form for finite-dimensional case as follow

$$(2.4) \quad q(x_1, \dots, x_M) = \prod_{j=1}^M q(x_j),$$

where $q(x_1, \dots, x_M)$ is the full probability density function, $q(x_j)$ is the probability density function for x_j , and $x_j \in \mathbb{R}^{N_j}$ ($N_j \in \mathbb{N}$) for $j = 1, 2, \dots, M$. That is to assume x_1, \dots, x_M are independent random variables with each other. By carefully chosen the random variables $\{x_j\}_{j=1}^M$, this independence assumption will lead to computational efficient solutions when conjugate prior probabilities are employed. For details, we refer to Chapter 9 in [6] and some recently published papers [26, 40, 41].

Inspired by formula (2.4), we need to specify the Banach space \mathcal{H} and subset \mathcal{A} as follow

$$(2.5) \quad \mathcal{H} = \prod_{j=1}^M \mathcal{H}_j, \quad \mathcal{A} = \prod_{j=1}^M \mathcal{A}_j,$$

where $\mathcal{A}_j \subset \mathcal{M}(\mathcal{H}_j)$, and M is a fixed positive constant. Let $\nu := \prod_{i=1}^M \nu^i$ represents a probability measure such that $\nu(dx) = \prod_{i=1}^M \nu^i(dx)$. With these assumptions, the minimization problem (2.3) can be rewritten as follow

$$(2.6) \quad \operatorname{argmin}_{\nu^i \in \mathcal{A}_i} D_{\text{KL}} \left(\prod_{i=1}^M \nu^i \parallel \mu \right)$$

for suitable sets \mathcal{A}_i with $i = 1, 2, \dots, M$. The general result shown in Proposition 2.1 indicates that the closedness of the subset \mathcal{A} under weak convergence is crucial for the existence of the approximate measure ν . Hence, we firstly present the following lemma, which illustrate the closedness of \mathcal{A} defined in (2.5).

Lemma 2.2. *For $i = 1, 2, \dots, M$, let $\mathcal{A}_i \subset \mathcal{M}(\mathcal{H}_i)$ be a series of sets closed under weak convergence of probability measures. Define*

$$(2.7) \quad \mathcal{C} := \left\{ \nu := \prod_{j=1}^M \nu^j \mid \nu^j \in \mathcal{A}_j \text{ for } j = 1, 2, \dots, M \right\}.$$

Then the set \mathcal{C} is closed under weak convergence of probability measures.

The proof details is postponed to the Appendix to keep the fluent presentation of the main ideas. From Lemma 2.2 and Proposition 2.1, we can conclude the following general existence result.

Theorem 2.3. *For $i = 1, 2, \dots, M$, let \mathcal{A}_i be closed with respect to weak convergence. For given $\mu \in \mathcal{M}(\prod_{i=1}^M \mathcal{H}_i)$, we assume that there exist $\nu^i \in \mathcal{A}_i$ such that $D_{\text{KL}}(\prod_{i=1}^M \nu^i \parallel \mu) < \infty$. Then, there exists a minimizer $\prod_{i=1}^M \nu^i$ solving problem (2.6).*

Remark 2.4. In Theorem 2.3, we only illustrate the existence of the approximate measure ν without uniqueness. When the approximate measures are assumed to be Gaussian, uniqueness has been obtained with λ -convex requirement of the potential Φ appeared in the Bayes' formula (2.1) [35]. Actually, we can not expect uniqueness generally even for most practical problems defined on finite-dimensional space. Hence, we will not pursue uniqueness result here.

The result shown in Theorem 2.3 does not tell us much about the manner in which minimizing sequences approach the limit. After some more work, we can actually characterize the convergence more precisely.

Theorem 2.5. *Let $\{\nu_n = \prod_{j=1}^M \nu_n^j\}_{n=1}^\infty$ be a sequence in $\prod_{j=1}^M \mathcal{M}(\mathcal{H}_j)$, and let $\nu_* = \prod_{j=1}^M \nu_*^j \in \prod_{j=1}^M \mathcal{M}(\mathcal{H}_j)$ and $\mu \in \mathcal{M}(\prod_{j=1}^M \mathcal{H}_j)$ be probability measures such that for any $n \geq 1$ we have $D_{\text{KL}}(\nu_n \parallel \mu) < \infty$ and $D_{\text{KL}}(\nu_* \parallel \mu) < \infty$. Suppose that ν_n converges weakly to ν_* and $\nu_n^j \ll \nu_*^j$ for $j = 1, 2, \dots, M$, and in addition that*

$$(2.8) \quad D_{\text{KL}}(\nu_n \parallel \mu) \rightarrow D_{\text{KL}}(\nu_* \parallel \mu).$$

Then ν_n^j converges to ν_^j in total variation norm for $j = 1, 2, \dots, M$.*

Combining Theorem 2.3 with Theorem 2.5, we immediately obtain the following result.

Corollary 2.6. *For $j = 1, 2, \dots, M$, let $\mathcal{A}_j \subset \mathcal{M}(\mathcal{H}_j)$ be closed with respect to weak convergence. For given $\mu \in \mathcal{M}(\prod_{j=1}^M \mathcal{H}_j)$, there exists a $\nu = \prod_{j=1}^M \nu^j \in \prod_{j=1}^M \mathcal{A}_j$ with $D_{KL}(\nu||\mu) < \infty$. Let $\nu_n = \prod_{j=1}^M \nu_n^j \in \prod_{j=1}^M \mathcal{A}_j$ satisfy*

$$(2.9) \quad D_{KL}(\nu_n||\mu) \rightarrow \inf_{\nu \in \prod_{j=1}^M \mathcal{A}_j} D_{KL}(\nu||\mu).$$

Then, after passing to a subsequence, ν_n converges weakly to a $\nu_ \in \prod_{j=1}^M \mathcal{M}(\mathcal{H}_j)$ that realizes the infimum in (2.9), and each component ν_n^j converges weakly to ν_*^j . If in addition $\nu_n^j \ll \nu_*^j$ for all n and $j = 1, 2, \dots, M$, we have ν_n^j converges to ν_*^j in total-variation norm.*

2.2. Mean-field approximation for functions. For the finite-dimensional case, the mean field approximation has been widely employed in the field of machine learning. Based on the results obtained in Subsection 2.1, we will construct a mean field approximation approach in infinite-dimensional space, which will be useful for inverse problems of PDEs.

In the infinite-dimensional setting, the Gaussian measure sometimes plays the role of Lebesgue measure. Inspired by Example 3.8 and 3.9 shown in [35] and the general setting given in [34], we may assume the approximate probability measure ν is equivalent to μ_0 defined by

$$(2.10) \quad \frac{d\nu}{d\mu_0}(x) = \frac{1}{Z_\nu} \exp(-\Phi_\nu(x)).$$

Compared with the finite-dimensional case, a natural way for introducing independence assumption is to assume that the potential $\Phi_\nu(x)$ can be divided as follow

$$(2.11) \quad \Phi_\nu(x) = \prod_{j=1}^M \Phi_\nu^j(x_j),$$

where $x = (x_1, \dots, x_M)$. However, this intuitive idea prevents us to incorporate parameters appeared in the prior probability measure into hierarchical Bayes' model which is broadly used in finite-dimensional case [26, 41]. Based on these considerations, we propose the following assumption that introduces a reference probability measure.

Assumption 2.7. *Let us introduce a reference probability measure*

$$(2.12) \quad \mu_r(dx) = \prod_{j=1}^M \mu_r^j(dx_j),$$

which is equivalent to the prior probability measure with the following relation holds true

$$(2.13) \quad \frac{d\mu_0}{d\mu_r}(x) = \frac{1}{Z_0} \exp(-\Phi^0(x)).$$

In addition, we assume that the approximate probability measure ν is equivalent to the reference measure μ_r , and the Radon-Nikodym derivative of ν with respect to

μ_r has the following form

$$(2.14) \quad \frac{d\nu}{d\mu_r}(x) = \frac{1}{Z_r} \exp \left(- \sum_{j=1}^M \Phi_j^r(x_j) \right).$$

Following Assumption 2.7, we know that the approximate measure can be decomposed as $\nu(dx) = \prod_{j=1}^M \nu^j(dx_j)$ with

$$(2.15) \quad \frac{d\nu^j}{d\mu_r^j} = \frac{1}{Z_r^j} \exp \left(- \Phi_j^r(x_j) \right).$$

Here, $Z_r^j = \mathbb{E}^{\mu_r^j} \left(\exp \left(- \Phi_j^r(x_j) \right) \right)$ ensures ν^j is indeed a probability measure. Obviously, we can define \mathcal{A}_j ($j = 1, 2, \dots, M$) as follow

$$\mathcal{A}_j = \left\{ \nu^j \in \mathcal{M}(\mathcal{H}_j) \mid \nu^j \text{ is equivalent to } \mu_r^j, \text{ and } \frac{d\nu^j}{d\mu_r^j} = \frac{1}{Z_r^j} \exp(-\Phi_j^r(x_j)) \right\}.$$

In order to use Theorem 2.3, we need to illustrate the closedness of \mathcal{A}_j ($j = 1, 2, \dots, M$) under the weak convergence topology. If each potential Φ_j^r has a lower and upper bound, and the reference measure satisfy some general conditions, we actually can prove the desired results shown below.

Lemma 2.8. *For each $j = 1, 2, \dots, M$, there exist a constant N such that*

$$(2.16) \quad \inf_{\nu^j \in \mathcal{A}_j} \Phi_j^r(x_j) \geq -N.$$

And for all $M > 0$, there exist a constant C_M related to M such that

$$(2.17) \quad \sup_{\|x_j\|_{\mathcal{H}_j} \leq M} \sup_{\nu^j \in \mathcal{A}_j} \Phi_j^r(x_j) \leq C_M < \infty.$$

Denote $T_{N_b}^j = \{x \mid \|x\|_{\mathcal{H}_j} \leq N_b\}$ with N_b be an arbitrary positive constant. Concerning the reference measure μ_r^j , we assume $\sup_{N_b} \mu_r^j(T_{N_b}^j) = 1$. Then, each \mathcal{A}_j is closed with respect to weak convergence.

With Lemma 2.8 at hand, we can easily obtain an existence result. In the following theorem, we provide a solution that facilitate us to obtain the optimal approximate measure via simple iterative updates.

Theorem 2.9. *Assume that the approximate probability measure in problem (2.6) satisfy Assumption 2.7, and the reference measure satisfy assumptions presented in Lemma 2.8, then problem (2.6) processes a solution with the following form*

$$(2.18) \quad \frac{d\nu}{d\mu_r} \propto \exp \left(- \sum_{i=1}^M \Phi_i^r(x_i) \right),$$

where

$$(2.19) \quad \Phi_i^r(x_i) = \int_{\prod_{j \neq i} \mathcal{H}_j} \left(\Phi^0(x) + \Phi(x) + \log Z_\mu + \log Z_0 \right) \prod_{j \neq i} \nu^j(dx_j) + \text{Const}$$

and

$$(2.20) \quad \nu^i(dx_i) \propto \exp \left(- \Phi_i^r(x_i) \right) \mu_r^i(dx_i).$$

Remark 2.10. Formula (2.19) means the logarithm of the optimal solution for factor ν^j is obtained simply by considering the logarithm of the joint distribution over all other variables and then taking the expectation with respect to all of the other factors $\{\nu^i\}$ for $i \neq j$. This result is in accordance with the finite-dimensional case illustrated in Subsection 2.3 of [40].

Remark 2.11. Based on Theorem 2.9, we can therefore seek a solution by first initializing all of the potentials Φ_j^r appropriately and then cycling through the potentials and replacing each in turn with a revised estimate given by the right-hand side of (2.19) evaluated using the current estimates for all of the other potentials.

3. APPLICATIONS TO SOME GENERAL INVERSE PROBLEMS

In Subsection 3.1, we apply our general theory to an abstract linear inverse problem (ALIP). We assume that the prior and noise probability measures are all Gaussian with some hyper-parameters, then we formulate hierarchical models which can be efficiently solved by variational Bayes' approach. In Subsection 3.2, we assume the noise distributed according to Laplace distribution. Through this assumption, we can formulate algorithms that solve ALIP robust to outliers. In Subsection 3.3, we give a brief discussion about nonlinear inverse problems.

3.1. Linear inverse problems with Gaussian noise. In this subsection, we apply our general theory to an abstract linear inverse problem. A detailed investigation for the corresponding finite-dimensional case can be found in [27].

Let \mathcal{H}_u be some separable Hilbert space and N_d be a positive integer, then we describe Bayesian method for linear inverse problem

$$(3.1) \quad d = Hu + \epsilon,$$

where $d \in \mathbb{R}^{N_d}$ is the measurement data, $u \in \mathcal{H}_u$ is the sought-for solution, H is a bounded linear operator from \mathcal{H}_u to \mathbb{R}^{N_d} , ϵ is a Gaussian random vector with mean zero and variance $\tau^{-1}I$. We will focus on hyper-parameter treatment within hierarchical models, and the challenges for exploring the posterior probability efficiently.

To formulate this problem in the Bayesian inverse framework, we should firstly introduce a prior probability measure for the unknown function u . Denote \mathcal{C}_0 be a symmetric, positive definite, and trace class operator defined on \mathcal{H}_u . Let (e_k, α_k) be eigen-system of the operator \mathcal{C}_0 such that $\mathcal{C}_0 e_k = \alpha_k e_k$, then, according to Subsection 2.4 in [16], we have

$$(3.2) \quad \mathcal{C}_0 = \sum_{j=1}^{\infty} \alpha_j e_j \otimes e_j,$$

where \otimes denotes tensor product on Hilbert space [36]. As indicated in [13, 14, 19], we assume that the data is only informative on a finite number of directions in \mathcal{H}_u . Under this assumption, we introduce a positive integer K , which represents the number of dimensions that are informed by the data (i.e., the so-called intrinsic dimensionality), which is different to the discretization dimensionality, i.e., the number of mesh points used to represent the unknown. Now, we define

$$(3.3) \quad \lambda^{-1} \mathcal{C}_0^K := \sum_{j=1}^K \lambda^{-1} \alpha_j e_j \otimes e_j + \sum_{j=N+1}^{\infty} \alpha_j e_j \otimes e_j,$$

which is obviously a symmetric, positive definite, and trace class operator. Then, we assume

$$(3.4) \quad u \sim \mu_0^{u,\lambda} = \mathcal{N}(u_0, \lambda^{-1} \mathcal{C}_0^K).$$

Denote $\text{Gamma}(\alpha, \beta)$ be the Gamma probability measure defined on \mathbb{R}^+ with the probability density function p_G has the following form

$$(3.5) \quad p_G(x; \alpha, \beta) = \frac{\beta^\alpha}{\Gamma(\alpha)} x^{\alpha-1} e^{-\beta x},$$

where $\Gamma(\cdot)$ is the usual Gamma function. Then, except for the function u , we assume that the parameters λ and τ appeared in the prior probability measure and noise probability measure are all random variables satisfy $\lambda \sim \mu_0^\lambda := \text{Gamma}(\alpha_0, \beta_0)$ and $\tau \sim \mu_0^\tau := \text{Gamma}(\alpha_1, \beta_1)$. With these preparations, we give the prior probability measure employed for this problem as follow

$$(3.6) \quad \mu_0(du, d\lambda, d\tau) = \mu_0^{u,\lambda}(du) \mu_0^\lambda(d\lambda) \mu_0^\tau(d\tau).$$

Denote μ be the posterior probability measure for random variables u , λ and τ , according to the theory exposed in [16], it can be defined as follow

$$(3.7) \quad \frac{d\mu}{d\mu_0}(u, \lambda, \tau) = \frac{1}{\tilde{Z}_\mu} \tau^{-N_d/2} \exp\left(-\frac{\tau}{2} \|Hu - d\|^2\right),$$

where

$$(3.8) \quad \tilde{Z}_\mu = \int_{\mathcal{H}_u \times \mathbb{R}^+ \times \mathbb{R}^+} \tau^{-N_d/2} \exp\left(-\frac{\tau}{2} \|Hu - d\|^2\right) \mu_0(du, d\lambda, d\tau).$$

Until now, the Bayes' formula for the abstract linear inverse problem has been established. For applying the general theory developed in Section 2, we should specify a reference probability measure. For this example, we choose the following reference measure

$$(3.9) \quad \mu_r(du, d\lambda, d\tau) = \mu_r^u(du) \mu_r^\lambda(d\lambda) \mu_r^\tau(d\tau),$$

where $\mu_r^u = \mathcal{N}(u_0, \mathcal{C}_0)$ is a Gaussian probability measure, μ_r^λ and μ_r^τ are chosen equal to μ_0^λ and μ_0^τ respectively.

As in Assumption 2.7, we assume that the approximate probability measure is separable with respect to the random variables u , λ and τ with the following form

$$(3.10) \quad \nu(du, d\lambda, d\tau) = \nu^u(du) \nu^\lambda(d\lambda) \nu^\tau(d\tau).$$

In addition, we assume that its Radon-Nikodym derivate with respect to μ_r can be written as

$$(3.11) \quad \frac{d\nu}{d\mu_r}(u, \lambda, \tau) = \frac{1}{Z_r} \exp\left(-\Phi_u^r(u) - \Phi_\lambda^r(\lambda) - \Phi_\tau^r(\tau)\right).$$

For the Radon-Nikodym derivative of μ_0 with respect to μ_r , we have

$$\begin{aligned}
 (3.12) \quad \frac{d\mu_0}{d\mu_r}(u, \lambda, \tau) &= \frac{d\mu_0^{u, \lambda}}{d\mu_r^u}(u) \frac{d\mu_0^\lambda}{d\mu_r^\lambda}(\lambda) \frac{d\mu_0^\tau}{d\mu_r^\tau}(\tau) \\
 &= \lambda^{K/2} \exp \left(-\frac{1}{2} \|(\lambda^{-1} \mathcal{C}_0^K)^{-1/2} (u - u_0)\|^2 + \frac{1}{2} \|\mathcal{C}_0^{-1/2} (u - u_0)\|^2 \right) \\
 &= \lambda^{K/2} \exp \left(-\frac{1}{2} \sum_{j=1}^K (u_j - u_{0j})^2 (\lambda - 1) \alpha_j^{-1} \right),
 \end{aligned}$$

which implies Φ^0 and Z_0 introduced in Assumption 2.7 have the following form

$$(3.13) \quad \Phi^0(u, \lambda, \tau) = \frac{1}{2} \sum_{j=1}^K (u_j - u_{0j})^2 (\lambda - 1) \alpha_j^{-1}, \quad Z_0 = \lambda^{-K/2}.$$

The reference probability measure employed here consists with three components that are one Gaussian measure accompanied with two Gamma measure. By choosing the space \mathcal{H}_u and the operator \mathcal{C}_0 carefully, we can ensure $\nu^u(\mathcal{H}_u) = 1$. Combining this with formula (3.13), we can verify the conditions in Lemma 2.8. According to (3.12) and (3.7), we find that $D_{\text{KL}}(\mu_r || \mu) < \infty$. By taking $\nu = \mu_r$, the above inequality verifies the conditions in Theorem 2.3. In summary, we can give the following theorem.

Theorem 3.1. *For a constant $N > 0$ and for all $M > 0$ there exists a constant C_M such that*

$$\begin{aligned}
 \mathcal{A}_u &= \left\{ \nu^u \in \mathcal{M}(\mathcal{H}_u) \left| \begin{array}{l} \nu^u \text{ is equivalent to } \mu_r^u, \quad \frac{d\nu^u}{d\mu_r^u} \propto \exp(-\Phi_u^r(u)) \\ \text{with } \Phi_u^r(u) \geq -N \text{ and } \sup_{\|u\|_{\mathcal{H}_u} \leq M} \Phi_u^r(u) \leq C_M \end{array} \right. \right\}, \\
 \mathcal{A}_\lambda &= \{ \nu^\lambda \in \mathcal{M}(\mathbb{R}^+) \mid \nu^\lambda = \mu_r^\lambda \}, \quad \mathcal{A}_\tau = \{ \nu^\tau \in \mathcal{M}(\mathbb{R}^+) \mid \nu^\tau = \mu_r^\tau \}.
 \end{aligned}$$

Let the approximate probability measure ν defined as in (3.10), and the posterior probability measure specified as in (3.7). Then there exists a minimizer ν solves the optimization problem $\min_{\nu \in \mathcal{A}} D_{\text{KL}}(\nu || \mu)$ with $\mathcal{A} = \prod_{j=u, \lambda, \tau} \mathcal{A}_j$.

Now, we are ready to calculate $\Phi_u^r(u)$, $\Phi_\lambda^r(\lambda)$ and $\Phi_\tau^r(\tau)$ according the general results shown in Theorem 2.9.

Calculate $\Phi_u^r(u)$: A direct application of formula (2.19) yields

$$\begin{aligned}
 (3.14) \quad \Phi_u^r(u) &= \int_0^\infty \int_0^\infty \left(\frac{1}{2} \sum_{j=1}^K (u_j - u_{0j})^2 (\lambda - 1) \alpha_j^{-1} + \frac{\tau}{2} \|Hu - d\|^2 \right. \\
 &\quad \left. - \frac{K}{2} \log \lambda - \frac{N_d}{2} \log \tau \right) \nu^\tau(d\tau) \nu^\lambda(d\lambda) + \text{Const} \\
 &= \frac{1}{2} \tau^* \|Hu - d\|^2 + \frac{1}{2} (\lambda^* - 1) \sum_{j=1}^K \alpha_j^{-1} (u_j - u_{0j})^2 + \text{Const},
 \end{aligned}$$

where

$$(3.15) \quad \tau^* = \mathbb{E}^{\nu^\tau}[\tau] = \int_0^\infty \tau \nu^\tau(d\tau) \quad \text{and} \quad \lambda^* = \mathbb{E}^{\nu^\lambda}[\lambda] = \int_0^\infty \lambda \nu^\lambda(d\lambda).$$

Relying on equality (3.14), we derive

$$(3.16) \quad \frac{d\nu^u}{d\mu_r^u}(u) \propto \exp\left(-\frac{\tau^*}{2}\|Hu - d\|^2 - \frac{\lambda^* - 1}{2} \sum_{j=1}^K \alpha_j^{-1} (u_j - u_{0j})^2\right).$$

Define

$$(3.17) \quad \mathcal{C}_0(\lambda^*) = \sum_{j=1}^K (\lambda^*)^{-1} \alpha_j e_j \otimes e_j + \sum_{j=K+1}^{\infty} \alpha_j e_j \otimes e_j.$$

Then, according to the Example 6.23 shown in [37], we know that the probability measure ν^u is a Gaussian measure $\mathcal{N}(u^*, \mathcal{C})$ with

$$(3.18) \quad \mathcal{C}^{-1} = \tau^* H^* H + \mathcal{C}_0(\lambda^*)^{-1} \quad \text{and} \quad u^* = \mathcal{C}(\tau^* H^* d + \mathcal{C}_0(\lambda^*)^{-1} u_0).$$

Calculate $\Phi_\lambda^r(\lambda)$ and $\Phi_\tau^r(\tau)$: According to formula (2.19), we have

$$(3.19) \quad \begin{aligned} \Phi_\lambda^r(\lambda) &= \int_0^\infty \int_{\mathcal{H}_u} \left(\frac{1}{2} \sum_{j=1}^K (u_j - u_{0j})^2 \alpha_j^{-1} \lambda - \frac{K}{2} \log \lambda \right) \nu^u(du) \nu^\tau(d\tau) + \text{Const} \\ &= \frac{1}{2} \mathbb{E}^{\nu^u} \left(\sum_{j=1}^K (u_j - u_{0j})^2 \alpha_j^{-1} \right) \lambda - \frac{K}{2} \log \lambda + \text{Const}, \end{aligned}$$

which implies

$$(3.20) \quad \frac{d\nu^\lambda}{d\mu_r^\lambda}(\lambda) \propto \lambda^{K/2} \exp\left(-\frac{1}{2} \mathbb{E}^{\nu^u} \left(\sum_{j=1}^K (u_j - u_{0j})^2 \alpha_j^{-1} \right) \lambda\right).$$

Because λ is a scalar random variable, we can write the density function as follow

$$(3.21) \quad \rho_G(\lambda; \tilde{\alpha}_0, \tilde{\beta}_0) = \frac{\tilde{\beta}_0^{\tilde{\alpha}_0}}{\Gamma(\tilde{\alpha}_0)} \lambda^{\tilde{\alpha}_0 - 1} \exp(-\tilde{\beta}_0 \lambda),$$

where

$$(3.22) \quad \tilde{\alpha}_0 = \alpha_0 + \frac{K}{2} \quad \text{and} \quad \tilde{\beta}_0 = \beta_0 + \frac{1}{2} \mathbb{E}^{\nu^u} \left(\sum_{j=1}^K (u_j - u_{0j})^2 \alpha_j^{-1} \right).$$

Similar to the above calculations of $\Phi_\lambda^r(\lambda)$, we can derive

$$(3.23) \quad \begin{aligned} \Phi_\tau^r(\tau) &= \int_0^\infty \int_{\mathcal{H}_u} \left(\frac{\tau}{2} \|Hu - d\|^2 - \frac{N_d}{2} \log \tau \right) \nu^u(du) \nu^\lambda(d\lambda) + \text{Const} \\ &= \frac{1}{2} \mathbb{E}^{\nu^u} (\|Hu - d\|^2) \tau - \frac{N_d}{2} \log \tau + \text{Const}, \end{aligned}$$

which implies

$$(3.24) \quad \frac{d\nu^\tau}{d\mu_r^\tau}(\tau) \propto \tau^{\frac{N_d}{2}} \exp\left(-\frac{1}{2} \mathbb{E}^{\nu^u} (\|Hu - d\|^2) \tau\right).$$

Hence, ν^τ is a Gamma distribution $\text{Gamma}(\tilde{\alpha}_1, \tilde{\beta}_1)$ with

$$(3.25) \quad \tilde{\alpha}_1 = \alpha_1 + \frac{N_d}{2} \quad \text{and} \quad \tilde{\beta}_1 = \beta_1 + \frac{1}{2} \mathbb{E}^{\nu^u} (\|Hu - d\|^2).$$

Combining (3.14), (3.22) and (3.25), we obviously find out that $\Phi_u^r(u)$ in the iterative procedure satisfy conditions proposed in Theorem 3.1. According to the

statements in Remark 2.11, we can provide an iterative algorithm based on formula (3.18), (3.21), (3.22) and (3.25) in Algorithm 1.

Algorithm 1 Variational approximation for the case of Gaussian noise

- 1: Give an initial guess $\mu_0^{u,\lambda}$ (u_0 and λ), μ_0^λ (α_0 and β_0) and μ_0^τ (α_1 and β_1).
Specify the tolerance tol and set $k = 1$.
 - 2: **repeat**
 - 3: Set $k = k + 1$
 - 3: Calculate $\lambda_k = \mathbb{E}^{\nu_{k-1}^\lambda}[\lambda]$, $\tau_k = \mathbb{E}^{\nu_{k-1}^\tau}[\tau]$
 - 4: Calculate ν_k^u by

$$\mathcal{C}_k^{-1} = \tau_k H^* H + \mathcal{C}_0(\lambda_k)^{-1}, \quad u_k = \mathcal{C}_k(\tau_k H^* d + \mathcal{C}_0(\lambda_k)^{-1} u_0).$$
 - 5: Calculate ν_k^λ and ν_k^τ by

$$\nu_k^\lambda = \text{Gamma}(\tilde{\alpha}_0, \tilde{\beta}_0^k), \quad \nu_k^\tau = \text{Gamma}(\tilde{\alpha}_1, \tilde{\beta}_1^k),$$
where

$$\tilde{\beta}_0^k = \beta_0 + \frac{1}{2} \mathbb{E}^{\nu_k^u} \left(\sum_{j=1}^K (u_j - u_{0j})^2 \alpha_j^{-1} \right), \quad \tilde{\beta}_1^k = \beta_1 + \frac{1}{2} \mathbb{E}^{\nu_k^u} (\|Hu - d\|^2).$$
 - 6: **until** $\|u_k - u_{k-1}\| / \|u_{k-1}\| \leq tol$
 - 7: Return $\nu_k^u(du) \nu_k^\lambda(d\lambda) \nu_k^\tau(d\tau)$ as the solution.
-

3.2. Linear inverse problems with Laplace noise. As indicated in the studies about low-rank matrix factorization [41], the Gaussian noise is sensitive to outliers. Compared with the Gaussian distribution, the Laplace distribution has a larger probability density function value at the tail part, and thus it is known as a *heavy-tailed* distribution that can better fit heavy noises and outliers. In this subsection, we develop VBM for linear inverse problem (3.1) with Laplace noise assumption.

For the noise vector $\epsilon = (\epsilon_1, \epsilon_2, \dots, \epsilon_{N_d})^T \in \mathbb{R}^{N_d}$, we assume that each component ϵ_i follows the Laplace distribution with zero mean

$$(3.26) \quad \epsilon_i \sim \text{Laplace}\left(0, \sqrt{\frac{\tau}{2}}\right)$$

with $\tau \in \mathbb{R}^+$. The probability density function of the above Laplace distribution is denoted by $p_L(\epsilon_i|0, \sqrt{\tau/2})$ that holds the following form

$$(3.27) \quad p_L(\epsilon_i|0, \sqrt{\tau/2}) = \sqrt{\frac{2}{\tau}} \exp\left(-\frac{|\epsilon_i|}{\sqrt{\tau/2}}\right).$$

Obviously, the Laplace distribution can be hardly employed for posterior inference within the variational Bayes' inference framework. A commonly utilized strategy will be employed here to reformulate it as Gaussian scale mixture with exponential distributed prior to the variance, as indicated in [2, 41]. Let $p_E(z|\tau)$ be the density function of an exponential distribution, that is

$$(3.28) \quad p_E(z|\tau) = \frac{1}{\tau} \exp\left(-\frac{z}{\tau}\right).$$

Then, we have

$$\begin{aligned}
 p_L\left(x|0, \sqrt{\frac{\tau}{2}}\right) &= \frac{1}{2} \sqrt{\frac{2}{\tau}} \exp\left(-\sqrt{\frac{2}{\tau}}|x|\right) \\
 (3.29) \quad &= \int_0^\infty \frac{1}{\sqrt{2\pi z}} \exp\left(-\frac{x^2}{2z}\right) \frac{1}{\tau} \exp\left(-\frac{z}{\tau}\right) dz \\
 &= \int_0^\infty p_N(x|0, z) p_E(z|\tau) dz.
 \end{aligned}$$

Substituting (3.26) into the above equation, we obtain

$$(3.30) \quad p_L(\epsilon_i|0, \sqrt{\tau/2}) = \int_0^\infty p_N(\epsilon_i|0, z_i) p_E(z_i|\tau) dz_i,$$

where $p_N(\epsilon_i|0, z_i)$ is the density function of a Gaussian measure on \mathbb{R} with mean zero and covariance z_i . Thus, we can impose a two-level hierarchical prior instead of a single-level Laplace prior, on each ϵ_i

$$(3.31) \quad \epsilon_i \sim \mathcal{N}(0, z_i), \quad z_i \sim \text{Exponential}(\tau).$$

For the prior probability measure of u , we set it as in Subsection 3.1 for the Gaussian noise case, that is

$$(3.32) \quad u \sim \mu_0^{u, \lambda} = \mathcal{N}(u_0, \lambda^{-1} C_0^K), \quad \lambda \sim \mu_0^\lambda = \text{Gamma}(\alpha_0, \beta_0).$$

Denote $w_i = z_i^{-1}$. Since $z_i \sim \text{Exponential}(\tau)$, we know that $w_i \sim \mu_0^{w_i}$ with $\mu_0^{w_i}$ is a probability distribution with the following probability density function

$$(3.33) \quad \frac{1}{\tau} \exp\left(-\frac{1}{\tau w_i}\right) \frac{1}{w_i^2}.$$

Denote W be a diagonal matrix with diagonal $w = \{w_1, w_2, \dots, w_{N_d}\}$, and denote

$$(3.34) \quad \mu_0^w = \prod_{i=1}^{N_d} \mu_0^{w_i}.$$

Combining (3.32) and (3.34), we obtain the full prior probability measure as follow

$$(3.35) \quad \mu_0(du, d\lambda, dw) = \mu_0^{u, \lambda}(du) \mu_0^\lambda(d\lambda) \mu_0^w(dw).$$

For the reference probability measure, we set $\mu_r(du, d\lambda, dw) = \mu_r^u(du) \mu_r^\lambda(d\lambda) \mu_r^w(dw)$, where $\mu_r^u = \mathcal{N}(u_0, C_0)$, $\mu_r^\lambda = \mu_0^\lambda$, and $\mu_r^w = \mu_0^w$. Calculating as in (3.12), we obtain

$$(3.36) \quad \Phi^0(u, \lambda, \tau) = \frac{1}{2} \sum_{j=1}^K (u_j - u_{0j})^2 (\lambda - 1) \alpha_j^{-1}, \quad Z_0 = \lambda^{-K/2}.$$

For the posterior probability measure, we have

$$(3.37) \quad \frac{d\mu}{d\mu_0}(u, \lambda, w) = \frac{1}{\tilde{Z}_\mu} |W|^{1/2} \exp\left(-\frac{1}{2} \|W^{1/2}(Hu - d)\|^2\right),$$

which implies $\Phi(u, \lambda, w) = \frac{1}{2} \|W^{1/2}(Hu - d)\|^2 - \frac{1}{2} \log |W|$ and $Z_\mu = \tilde{Z}_\mu |W|^{-1/2}$. Finally, we specify the approximate probability measure as follow

$$(3.38) \quad \frac{d\nu}{d\mu_r}(u, \lambda, \tau) = \frac{1}{Z_r} \exp\left(-\Phi_u^r(u) - \Phi_\lambda^r(\lambda) - \Phi_\tau^r(\tau)\right).$$

Similar to Theorem 3.1 for the Gaussian noise case, the existence of minimizer can also be formalized to a theorem in the Laplace noise case. Here we omit the

details for conciseness. With these preparations, we are ready to calculate all of the three potentials appeared in (3.38).

Calculate Φ_u^r : Following formula (2.19), we derive

$$(3.39) \quad \begin{aligned} \Phi_u^r(u) &= \iint \frac{1}{2} \sum_{j=1}^K (u_j - u_{0j})^2 (\lambda - 1) \alpha_j^{-1} + \frac{1}{2} \|W^{1/2}(Hu - d)\|^2 d\nu^\lambda d\nu^w + \text{Const} \\ &= \frac{\lambda^* - 1}{2} \sum_{j=1}^K \alpha_j^{-1} (u_j - u_{0j})^2 + \frac{1}{2} \|W^*(Hu - d)\|^2 + \text{Const}, \end{aligned}$$

where $\lambda^* = \mathbb{E}^{\nu^\lambda}[\lambda]$ and $W^* = \text{diag}(\mathbb{E}^{\nu^w}[w_1], \mathbb{E}^{\nu^w}[w_2], \dots, \mathbb{E}^{\nu^w}[w_{N_d}])$. From equality (3.39), we easily conclude that

$$(3.40) \quad \frac{d\nu^u}{d\mu_r^u}(u) \propto \exp \left(-\frac{1}{2} \|(W^*)^{1/2}(Hu - d)\|^2 - \frac{\lambda^* - 1}{2} \sum_{j=1}^K \alpha_j^{-1} (u_j - u_{0j})^2 \right),$$

which implies that u distributed according to a Gaussian measure with covariance operator and mean value specified as $\mathcal{C}^{-1} = H^*W^*H + \mathcal{C}_0(\lambda^*)^{-1}$ and $u^* = \mathcal{C}(H^*W^*d + \mathcal{C}_0(\lambda^*)^{-1}u_0)$.

Calculate Φ_λ^r : Following formula (2.19), we derive

$$(3.41) \quad \begin{aligned} \Phi_\lambda^r(\lambda) &= \iint \frac{1}{2} \sum_{j=1}^K (u_j - u_{0j})^2 \alpha_j^{-1} \lambda - \frac{K}{2} \log \lambda d\nu^u d\nu^w + \text{Const} \\ &= \frac{1}{2} \mathbb{E}^{\nu^u} \left(\sum_{j=1}^K (u_j - u_{0j})^2 \alpha_j^{-1} \right) \lambda - \frac{K}{2} \log \lambda + \text{Const}. \end{aligned}$$

Hence, we have

$$(3.42) \quad \frac{d\nu^\lambda}{d\mu_r^\lambda}(\lambda) \propto \lambda^{K/2} \exp \left(-\frac{1}{2} \mathbb{E}^{\nu^u} \left(\sum_{j=1}^K (u_j - u_{0j})^2 \alpha_j^{-1} \right) \lambda \right),$$

which implies that ν^λ is a Gamma distribution, denoted by $\text{Gamma}(\tilde{\alpha}_0, \tilde{\beta}_0)$ with

$$(3.43) \quad \tilde{\alpha}_0 = \alpha_0 + K/2, \quad \tilde{\beta}_0 = \beta_0 + \frac{1}{2} \mathbb{E}^{\nu^u} \left(\sum_{j=1}^K (u_j - u_{0j})^2 \alpha_j^{-1} \right).$$

Calculate Φ_w^r : Following formula (2.19), we derive

$$(3.44) \quad \begin{aligned} \Phi_w^r(w) &= \iint \frac{1}{2} \|W^{1/2}(Hu - d)\|^2 - \frac{1}{2} \log |W| d\nu^u d\nu^\lambda + \text{Const} \\ &= \frac{1}{2} \sum_{j=1}^{N_d} \mathbb{E}^{\nu^u} [(Hu - d)_j^2] w_j - \frac{1}{2} \sum_{j=1}^{N_d} \log w_j + \text{Const}, \end{aligned}$$

which implies

$$(3.45) \quad \frac{d\nu^w}{d\mu_r^w}(w) \propto \prod_{j=1}^{N_d} w_j^{1/2} \exp \left(-\frac{1}{2} \mathbb{E}^{\nu^u} [(Hu - d)_j^2] w_j \right).$$

Because w is a finite dimensional random variable, we find that

$$\begin{aligned}
 d\nu^w &\propto \prod_{j=1}^{N_d} w_j^{1/2} \exp\left(-\frac{1}{2}\mathbb{E}^{\nu^u}[(Hu-d)_j^2]w_j\right) \frac{1}{\tau} \exp\left(-\frac{1}{\tau w_j}\right) \frac{1}{w_j^2} dw \\
 &\propto \prod_{j=1}^{N_d} \frac{1}{\tau w_j^{3/2}} \exp\left(-\frac{1}{2}\mathbb{E}^{\nu^u}[(Hu-d)_j^2]w_j - \frac{1}{\tau w_j}\right) dw.
 \end{aligned}
 \tag{3.46}$$

That is to say, ν^w is an inverse Gaussian distribution, denoted by $\prod_{j=1}^{N_d} IG(\mu_{w_j}, \zeta)$ with

$$\mu_{w_j} = \sqrt{\frac{2}{\tau \mathbb{E}^{\nu^u}[(Hu-d)_j^2]}}, \quad \zeta = \frac{2}{\tau}.
 \tag{3.47}$$

Specify the parameter τ : From (3.31), we know that the parameter τ is directly related to the noise variance parameter $z_i = w_i^{-1}$. Therefore, it should be adjusted carefully to obtain reasonable results. Empirical Bayes [6] provides an off-the-shelf tool to adaptively tuned based on the noise information extracted from data, by updating it through $\tau = \frac{1}{N_d} \sum_{j=1}^{N_d} \mu_{w_j}^{-1} + \zeta^{-1}$. Using this elaborate tool, τ can be properly adapted to real data variance.

Similar to the Gaussian noise case, an iterative algorithm, namely Algorithm 2, is constructed based on the above calculations.

Algorithm 2 Variational approximation for the case of Laplace noise

- 1: Give an initial guess $\mu_0^{u,\lambda}$ (u_0 and λ), μ_0^λ (α_0 and β_0), μ_0^w and τ .
Specify the tolerance tol and set $k = 1$.
- 2: **repeat**
- 3: Set $k = k + 1$
- 3: Calculate $\lambda_k = \mathbb{E}^{\nu_{k-1}^\lambda}[\lambda]$, $W_k = \text{diag}(\mathbb{E}^{\nu^w}[w_1], \mathbb{E}^{\nu^w}[w_2], \dots, \mathbb{E}^{\nu^w}[w_{N_d}])$
and
 $\tau_k = \frac{1}{N_d} \sum_{j=1}^{N_d} (\mu_{w_j}^{k-1})^{-1} + (\zeta_{k-1})^{-1}$.
- 4: Calculate ν_k^u by
 $\mathcal{C}_k^{-1} = H^* W_k H + \mathcal{C}_0(\lambda_k)^{-1}$, $u_k = \mathcal{C}_k(H^* W_k d + \mathcal{C}_0(\lambda_k)^{-1} u_0)$.
- 5: Calculate ν_k^λ and ν_k^w by

$$\nu_k^\lambda = \text{Gamma}(\tilde{\alpha}_0, \tilde{\beta}_0^k), \quad \nu_k^w = \prod_{j=1}^{N_d} IG(\mu_{w_j}^k, \zeta_k),$$

$$\tilde{\beta}_0^k = \beta_0 + \frac{1}{2} \mathbb{E}^{\nu_k^u} \left(\sum_{j=1}^K (u_j - u_{0j})^2 \alpha_j^{-1} \right), \quad \tilde{\alpha}_0 = \alpha_0 + K/2,$$

$$\mu_{w_j}^k = \sqrt{\frac{2}{\tau_k \mathbb{E}^{\nu_k^u}[(Hu-d)_j^2]}}, \quad \zeta_k = \frac{2}{\tau_k}.$$

- 6: **until** $\|u_k - u_{k-1}\| / \|u_{k-1}\| \leq tol$
 - 7: Return $\nu_k^u(du) \nu_k^\lambda(d\lambda) \nu_k^w(dw)$ as the solution.
-

3.3. Brief discussions about nonlinear problems. In practice, many inverse problems are described by nonlinear forward models, e.g., inverse medium scattering problem. For the finite-dimensional case, there are already some studies for VBM with nonlinear model, see e.g., the recent works [11, 26] and references therein.

Because calculating the KL divergence for general nonlinear forward models is analytically intractable, we can approximate the nonlinear forward model $H(u)$ by its first-order Taylor expansion $\tilde{H}(u)$ around the mode \tilde{u} of the posterior distribution, i.e., $\tilde{H}(u) = H(\tilde{u}) + H'(\tilde{u})(u - \tilde{u})$ with $H'(\tilde{u})$ is the Fréchet derivative of H at \tilde{u} . With this linearization available, we can recalculate every potential similar as in Subsection 3.1 and 3.2. Except linearization method, randomized optimization mentioned in Section 2.2 in [9, 10] may also be employed to calculate the expectations concerned with the sought-for solution u . Detailed studies for nonlinear problems are not the main point here, and investigations in this direction will be reported in our future work.

4. CONCRETE NUMERICAL EXAMPLES

4.1. Inverse source problem for Helmholtz equation. The inverse source problem (ISP) studied in this section is brought from [4, 5, 12, 23], which determines the unknown current density function from measurements of the radiated fields at multiple wavenumbers.

Consider the Helmholtz equation

$$(4.1) \quad \Delta v + \kappa^2(1 + q(x))v = u_s \quad \text{in } \mathbb{R}^{N_s},$$

where $N_s = 1, 2$ is the space dimension, κ is the wavenumber, v is the radiated scalar field, and the source current density function $u_s(x)$ is assumed to have a compact support. For the one-dimensional case, let the radiated field v satisfies the absorbing boundary condition: $\partial_r v = i\kappa v$. For the two-dimensional case, let the radiated field v satisfies the Sommerfeld radiation condition: $\partial_r v - i\kappa v = o(r^{-1/2})$ as $r = |x| \rightarrow \infty$. In addition, we employ an uniaxial PML technique to truncate the whole plane into a bounded rectangular domain when $N_s = 2$. For details of the uniaxial perfect match layer (PML) technique, we refer to [3, 25] and references therein. Let D be the domain with absorbing layers, and Ω be the physical domain without absorbing layers.

The ISP is to determine the source function u_s from the boundary measurements of the radiated field on the boundary $\partial\Omega$ for a series of wavenumbers. For clarity, we summarize the problem as follow:

Available data: For $0 < \kappa_1 < \kappa_2 < \cdots < \kappa_{N_f} < \infty$ ($N_f \in \mathbb{N}^+$), and measurement points $x^1, x^2, \dots, x^{N_m} \in \partial\Omega$, we denote

$$d^\dagger := \{v(x^i, \kappa_j) \mid i = 1, 2, \dots, N_m, \text{ and } j = 1, 2, \dots, N_f\}.$$

The available data is $d := d^\dagger + \epsilon$, where ϵ is measurement error.

Unknown function: The source density function u_s needs to be determined.

Generally, we let \mathcal{F}_κ be the forward operator maps u_s to the solution v when wavenumber is κ , and let \mathcal{M} be the measurement operator maps v to the available data. With these notations, the problem can be write abstractly as

$$(4.2) \quad d = H_\kappa(u_s) + \epsilon,$$

where $H_\kappa := \mathcal{M} \circ \mathcal{F}_\kappa$ is the forward operator, and ϵ is the random noise.

In order to avoid inverse crime, we use a fine mesh to generate data and a rough mesh for inversion. For the one-dimensional problem, meshes with mesh number equal to 1000 and 600 are used for data generation and inversion respectively. For the two-dimensional problem, we will provide details in the sequel.

At last, we should mention that the finite element method is implemented by employing an open software called FEniCS (Version 2018.1.0). For more about FEniCS, we refer to a book [31]. All the programs were run on the personal computer with Intel(R) Core(TM) i7-7700 at 3.60 GHz (CPU), 32 GB (memory), and Ubuntu 18.04.2 LTS (OS).

4.2. One-dimensional ISP. For clarity, let us firstly list the specific choices for some parameters introduced in Section 3 as follow:

- The operator \mathcal{C}_0 is chosen to be $(\text{Id} - \partial_{xx})^{-1}$. Here, the Laplace operator is defined on Ω with zero Dirichlet boundary condition;
- Wavenumber series are specified as $\kappa_j = j$ with $j = \frac{1}{2}, 1, \frac{3}{2}, 2, \dots, 50$.
- Let domain Ω be an interval $[0, 1]$, with $\partial\Omega = \{0, 1\}$. And the available data is assumed to be $\{v(x^i, \kappa_j) \mid i = 1, 2, x^1 = 0, x^2 = 1, \text{ and } j = 1, 2, \dots, 100\}$.
- The initial values required by Algorithm 1 are chosen as $u_0 = 0, \alpha_0 = \alpha_1 = 1, \beta_0 = 10^{-1}, \beta_1 = 10^{-5}$. The initial values required by Algorithm 2 are chosen as $u_0 = 0, \alpha_0 = 1, \beta_0 = 10^{-1}, \tau = 10^{-7}$.
- Considering Theorem 3.1 presented in [4], we believe that the parameter K should be extremely large for inverse source problem. So we set K equal to the dimensions of the discrete source.
- The function $q(x)$ in Helmholtz equation is taken to be constant zero.
- The ground truth source function u_s is defined as follow:

$$u_s(x) = 0.5 \exp(-300(x - 0.4)^2) + 0.5 \exp(-300(x - 0.6)^2).$$

According to the studies shown in [30], for this simple one-dimensional case, we will not take a recursive strategy here but combine all the data together with the forward operator denoted by \mathcal{H} defined by $H = (H_{\kappa_1}, H_{\kappa_2}, \dots, H_{\kappa_{100}})^T$. Based on these settings, we will provide some basic theoretical properties of the prior and posterior sampling functions as follow:

- The prior probability measure for u_s is Gaussian with covariance operator $\lambda^{-1}\mathcal{C}_0^K$ with $\lambda \in \mathbb{R}^+$. According to Theorem 12 illustrated in [16], we know that if u_s draws from the prior measure then

$$u_s \in W^{t,2}(\Omega) \quad \text{for } t < \frac{1}{2}, \quad \text{and} \quad u_s \in C^{0,t}(\Omega) \quad \text{for } t < \min\left(1, \frac{1}{2}\right),$$

where $W^{t,2}(\Omega)$ is the usual Sobolev space with t times derivative belong to $L^2(\Omega)$, and $C^{0,t}$ is the conventional Hölder space.

- For Algorithm 1, every posterior mean estimate u_k has the following form

$$u_k = (\tau_k H^* H + \mathcal{C}_0(\lambda_k)^{-1})^{-1} \tau_k H^* d.$$

Since H maps a function in $L^2(\Omega)$ to \mathbb{R}^{200} , we know that H^*d is at least a function belongs to L^2 . Considering the specific choices of \mathcal{C}_0 , we have $u_k \in W^{2,2}(\Omega)$. For Algorithm 2, we have similar conclusions.

Remark 4.1. By employing “Bayesian-then-discretize” method, we can analyze the prior and posterior sampling functions rigorously. It is one of the advantages for employing the proposed infinite-dimensional VBM.

Gaussian noise case: Denote d^\dagger be the data without noise. Then we add noises by $d = d^\dagger + \sigma\xi$ with $\sigma = 10^{-3}$ and ξ be a random variable sampled from the standard normal distribution.

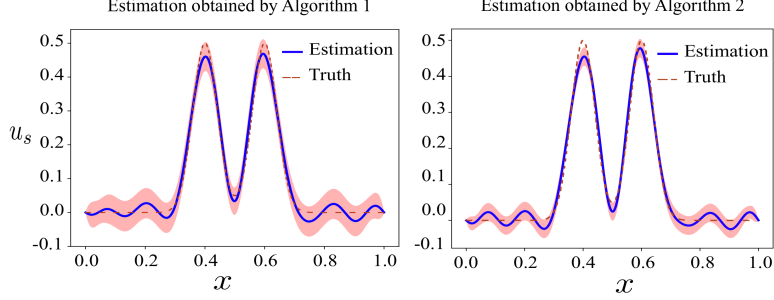


FIGURE 1. The truth and the estimated function when the data is polluted by Gaussian noise. Left panel: the estimated function obtained by Algorithm 1 is drawn by blue solid line, and the truth is drawn by red dashed line; Right panel: the estimated function obtained by Algorithm 2 is drawn by blue solid line, and the truth is drawn by orange dashed line; In both plots the shaded area represents the pointwise mean plus and minus two time the standard deviation (roughly corresponding to the 95% confidence region).

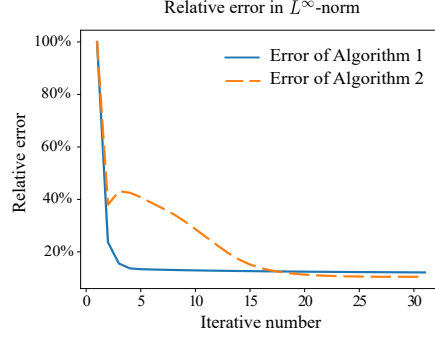


FIGURE 2. Relative error in L^∞ -norm of Algorithm 1 and 2.

In Figure 1, we present the truth and the estimated source obtained by Algorithm 1 and 2. Visually, the two algorithms provide reasonable results. In addition, we show 95% confidence region by shaded area to display the uncertainties estimated by the two algorithms. The truth is totally falling into the confidence region given by Algorithm 1, and most part of the truth lies in the confidence region given by Algorithm 2. This may reflect that for the Gaussian noise case Algorithm 1 can provide a more reliable estimation, which is in accordance with our assumptions.

In order to give a more careful comparison, we show the relative errors in L^∞ -norm of the two algorithms in Figure 2. The blue solid line and the orange dashed line are relative errors of Algorithm 1 and 2 respectively. Obviously, the two algorithms can provide comparable results after convergence. However, Algorithm 1 converges much faster than Algorithm 2. This is reasonable since the weight parameters used for detecting impulsive noises may reduce the convergence speed.

The parameter τ given by Algorithm 1 provides an estimate of the noise variance through the formula $\sigma = \sqrt{\tau^{-1}}$. The true value of σ is 0.001 in our numerical example. For providing a repeatable results, we specify the random seeds in numpy to some certain numbers by `numpy.random.seed(i)` with i equal to some integers. The estimated σ are equal to 0.000953, 0.001101, 0.001022, 0.001003 and 0.001041 when the random seed are specified as 1, 2, 3, 4, 5 respectively, which obviously illustrate the effectiveness of the proposed algorithm.

Laplace noise case: As for the Gaussian noise case, let d^\dagger be the noise-free measurement. The noisy data is generated as follow

$$d_i = \begin{cases} d_i^\dagger, & \text{with probability } 1 - r, \\ d_i^\dagger + \epsilon\xi, & \text{with probability } r, \end{cases}$$

where ξ follow the uniform distribution $U[-1, 1]$, and (ϵ, r) control the noise pattern: r is the corruption percentage and ϵ is the corruption magnitude. In the following, we take $r = 0.5$ and $\epsilon = 0.1$. In Figure 3, we plot the clean data and the noisy data, which visually illustrates the clean data is heavily polluted.

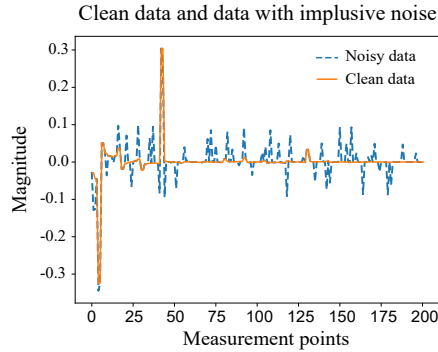


FIGURE 3. The orange solid line represents the clean data, and the blue dashed line represents data with impulsive noise.

In Figure 4, we show the estimated functions obtained by Algorithm 1 and 2 in the left panel and right panel respectively. Obviously, based on Gaussian noise assumption, Algorithm 1 can not provide a reasonable estimate, and the estimated confidence region may also unreliable. However, based on Laplace noise assumption, Algorithm 2 provides an accurate estimate. Since Algorithm 1 totally fail to converge to a reasonable estimation, we only provide the relative errors in L^∞ -norm of Algorithm 2 in the left panel of Figure 5. From these relative errors, we can find that Algorithm 2 converges very quickly even the data is heavily polluted by noises. In the right panel of Figure 5, we plot the noisy data and clean data points at the data points where noises are added. In addition, we plot the weight vector at the corresponding data points. From this figure, we clearly see that the

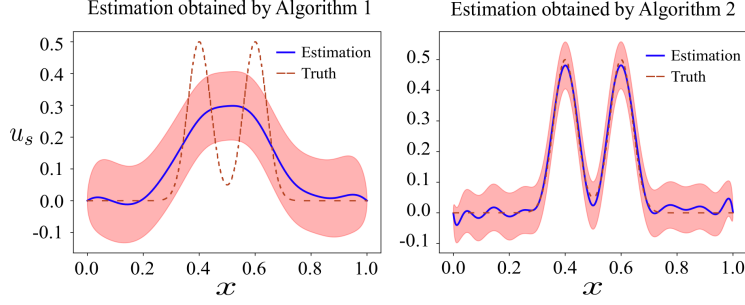


FIGURE 4. The truth and the estimated function when the data is polluted by impulsive noise. Left panel: The estimated function obtained by Algorithm 1 is drawn by blue solid line, and the truth is drawn by orange dashed line; Right panel: The estimated function obtained by Algorithm 2 is drawn by blue solid line, and the truth is drawn by red dashed line; The shaded areas in both panels represent the pointwise mean plus and minus two time the standard deviation (roughly corresponding to the 95% confidence region).

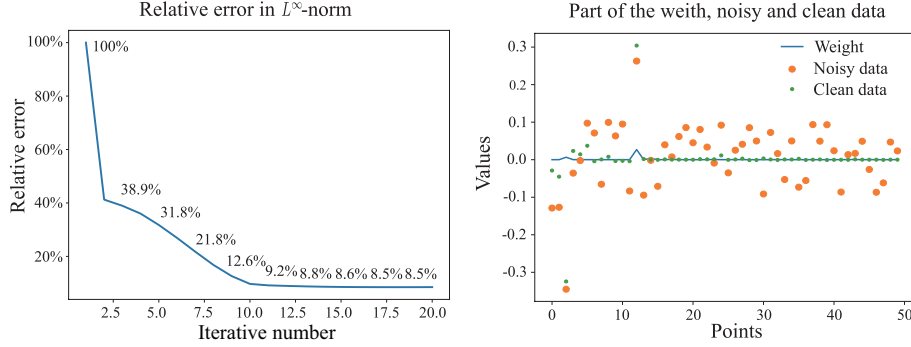


FIGURE 5. Left panel: Relative errors in L^∞ -norm obtained by Algorithm 2; Right panel: Weight, noisy and clean data at the data points with impulsive noise.

elements of the weight vector are all take small values, which just in accordance with our theory: the weight vectors at the noisy data points will be adjusted to zero during the iteration. This reveals the outlier removal mechanism of Algorithm 2.

4.3. Two-dimensional ISP. In this subsection, we solve two-dimensional ISP. For the two-dimensional problem, it seems hardly to compute the covariance operator directly due to the large memory requirements and computational inefficiency. Here, we employ a simple method that is using a rough mesh approximation to compute the covariance. The source function u_s can be expanded under basis

functions

$$(4.3) \quad u_s(x) = \sum_{i=1}^{\infty} u_{si} \varphi_i(x).$$

The basis functions can be taken as the finite element basis, so the source function can be approximated as follow

$$(4.4) \quad u_s(x) \approx \sum_{i=1}^{N_t} u_{si} \varphi_i(x).$$

The covariances appeared in Algorithm 1 and 2 are all computed by taking a small N_t in (4.4). Since for many applications, e.g., medical imaging, we may compute the operator H^*H (not depends on the source function) with small N_t before the inversion. For keeping evaluate accuracy as wavenumber increases, we employ a hybrid method: compute the mean function by gradient descent with a fine mesh discrete PDE solver, then project the source function to the rough mesh for computing variables relying on the covariance operators. Different to the one-dimensional case, we employ a sequential method that is used in [4]. Iteration details are presented in Algorithm 3.

Algorithm 3 VBM for two-dimensional ISP with multi-frequencies

- 1: Give an initial guess of the unknown source u_s , denoted by u_s^0 .
 - 2: For i from 1 to N_f (iterate from low wavenumber to high wavenumber)
 - 3: In the first iteration of Algorithm 1 or 2: rough approximate source is employed, and the prior mean is specified as u_s^{i-1} .
 - 4: For the remaining iterations of Algorithm 1 or 2: the mean value of $\mu_0^{u,\lambda}$ is specified as u_s^{i-1} , and the gradient descent method is employed to generate u_s^i on a fine mesh.
 - 5: End for
 - 6: Return the approximate probability measure ν .
-

In the following, if we said Algorithm 1 is employed, it is actually means Algorithm 3 combined with Algorithm 1 is employed. Similarly, Algorithm 2 is employed implies that Algorithm 3 combined with Algorithm 2 is employed.

Remark 4.2. Computing the covariance operator is equivalent to the problem of computing Hessian operator. This is a notoriously difficult problem encountered in many studies, e.g., Newton type method for PDE-constrained optimization problem [32], conduct uncertainty quantification for inverse problems [7]. Here, we will not pursuit this in detail. Efficient approximate of the covariances and applying the proposed algorithms to large-scale problems will be reported in our future studies.

Remark 4.3. In Algorithm 3, we use approximations on rough mesh for the first iteration of every wavenumber, which may provide an initial inaccurate adjust for parameters employed in Algorithm 1 and 2. In our numerical experiments, we only take two iterations for the fourth step to obtain an estimation.

Remark 4.4. For employing sampling type methods, i.e., MCMC algorithm, we must parameterize the unknown source function carefully to reduce the dimension. Even for a low dimensional problem, a large number of samples may needed for each

wavenumber [13, 19], which is usually unacceptable for ISP. The proposed Algorithm 3 will take several times of computational time compared with the classical iterative algorithm [4, 5, 22]. However, the proposed algorithm is relatively fast compared with the sampling method and, in addition, dimension reduction may not necessary.

Before going further, let us list the specific choices for some parameters introduced in Section 3 as follow:

- The operator \mathcal{C}_0 is chosen as $(-\Delta + \text{Id})^{-2}$. Here, the Laplace operator is defined on Ω with zero Dirichlet boundary condition;
- Take the discrete truncate level $N_t = 1681$, and the number of measurement points $N_m = 200$. The basis functions $\{\varphi_j\}_{j=1}^\infty$ are specified as the second-order finite element basis functions. Based on similar considerations for one-dimensional problem, we set K equal to the dimensions of the discrete source.
- For Algorithm 3 combined with Algorithm 1, wavenumber series are specified as $\kappa_j = j$ with $j = 1, 3, 5, \dots, 35$. For Algorithm 3 combined with Algorithm 2, wavenumber series are specified as $\kappa_j = j$ with $j = 1, 2, 3, \dots, 35$.
- To avoid inverse crime, a mesh with mesh number equal to 125000 is employed for generating data. Concerned with the inversion, two types of mesh are employed: a mesh with mesh number equal to 28800 is employed when wavenumbers are below 20; a mesh with mesh number equal to 41472 is employed when wavenumbers are larger than 20.
- The scatterer function $q(x)$ is defined as follow

$$\begin{aligned} q(x_1, x_2) = & 0.3(4 - 3x_1)^2 e^{(-9(x_1-1)^2 - 9(x_2-2/3)^2)} \\ & - (0.6(x_1 - 1) - 9(x_1 - 1)^3 - 3^5(x_2 - 1)^5) e^{(-9(x_1-1)^2 - 9(x_2-1)^2)} \\ & - 0.03e^{-9(x_1-2/3)^2 - 9(x_2-1)^2}, \end{aligned}$$

which is the function used in Subsection 2.6 in [4].

- The true source function u_s is defined as follow:

$$u_s(x) = 0.5e^{-100((x_1-0.7)^2 + (x_2-1)^2)} + 0.3e^{-100((x_1-1.3)^2 + (x_2-1)^2)}.$$

The case of Gaussian noise: Denote d^\dagger be the data without noise. The synthetic noisy data d are generated by $d_j = d_j^\dagger + \sigma \xi_j$, where $\sigma = \max_{1 \leq j \leq N_m} \{|d_j^\dagger|\} L_{\text{noise}}$ with L_{noise} denotes the relative noise level, and ξ_j are standard normal random variables. In our experiments, we take $L_{\text{noise}} = 0.05$, that is to say, 5% percentage of noises are added.

In Figure 6, we show the true source, posterior mean estimates obtained by Algorithm 1 and 2 on the left, middle and right panel respectively. Visually, there are no large differences between the two estimates, and all of the two estimations are similar to the truth. In Figure 7, we show the relative errors in L^∞ -norm obtained by Algorithm 1 and 2 on the left and right panel respectively. As the wavenumber increases, the relative errors obtained by both algorithms are decrease quickly. However, let us recall that more wavenumbers are used for Algorithm 2. If the wavenumber series $\kappa_j = j$ ($j = 1, 3, 5, \dots, 35$) are employed for Algorithm 2, the final relative error in L^∞ -norm will be 26.05% (higher than the present value 14.40%), which reflects that Algorithm 2 converges slower than Algorithm 1.

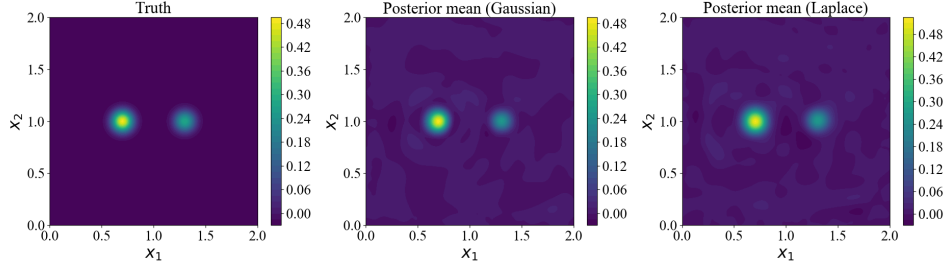


FIGURE 6. Left panel: The true source function; Middle panel: The posterior mean estimate obtained by Algorithm 3 combined with Algorithm 1; Right panel: The posterior mean estimate obtained by Algorithm 3 combined with Algorithm 2.

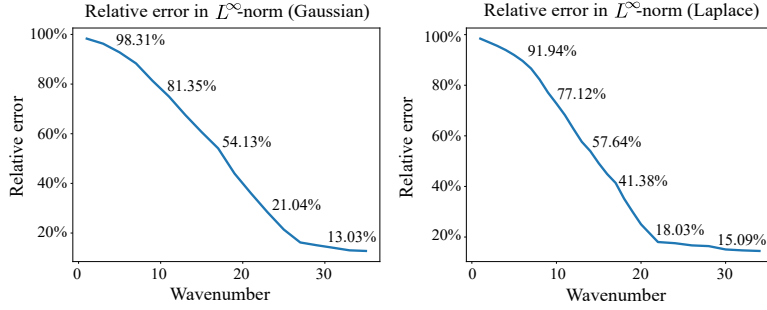


FIGURE 7. Left panel: Relative errors in L^∞ -norm obtained by Algorithm 3 combined with Algorithm 1; Right panel: Relative errors in L^∞ -norm obtained by Algorithm 3 combined with Algorithm 2.

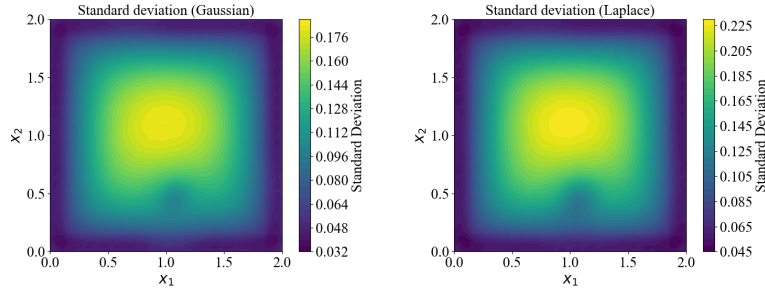


FIGURE 8. Standard deviation of the numerical solution obtained by different algorithms. Left panel: Estimated standard deviation obtained by Algorithm 3 combined with Algorithm 1; Right panel: Estimated standard deviation obtained by Algorithm 3 combined with Algorithm 2.

In Figure 8, we show the standard deviations (std) obtained by Algorithm 1 and Algorithm 2 in the left and right panel respectively. Obviously, Algorithm 1 provides tighter standard deviations for the numerical solution, which may implies that the posterior mean provided by Algorithm 1 is more reliable compared with the estimate provided by Algorithm 2.

In summary, both of Algorithm 1 and 2 provide an acceptable posterior mean estimate and an estimate of the standard deviation. If the data is polluted by small Gaussian noise, Algorithm 1 will be more computationally efficient.

The case of Laplace noise: As for the Gaussian noise case, let d^\dagger be the noise-free measurement. The noisy data are generated as follow

$$d_i = \begin{cases} d_i^\dagger, & \text{with probability } 1 - r, \\ d_i^\dagger + \epsilon\xi, & \text{with probability } r, \end{cases}$$

where ξ follow the uniform distribution $U[-1, 1]$, and (ϵ, r) control the noise pattern: r is the corruption percentage and ϵ is the corruption magnitude defined by $\epsilon = \max_{1 \leq j \leq N_m} \{|d_j^\dagger|\} L_{\text{noise}}$ with L_{noise} denotes the relative noise level. In our experiments, we take $L_{\text{noise}} = 1$ and $r = 0.2$ or 0.5 .

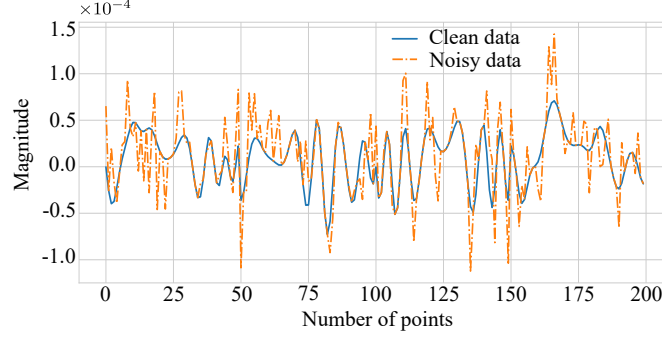


FIGURE 9. Clean and noisy data obtained when the wavenumber is 34. The blue solid line represents clean data and the dashed orange line represents noisy data with $r = 0.5$.

Firstly, we visually show the noisy and clean data when the wavenumber is equal to 34 and $r = 0.5$ in Figure 9. Obviously, the data are heavily contaminated by noise. Actually, Algorithm 1 can not provide an acceptable results and totally failed under this setting. In Figure 10, we show the true source function, the posterior mean estimates generated by Algorithm 2 when $r = 0.2$ and $r = 0.5$ on the left, middle and right panel respectively. Visually, there are no big differences for the posterior mean estimates when $r = 0.2$ and $r = 0.5$. However, Bayes' method not only provides point estimates, e.g., posterior mean estimates, but also tells us the reliability of the obtained estimations. In Figure 11, we show the standard deviations provided by Algorithm 2 when $r = 0.2$ and $r = 0.5$ on the left and right panel respectively. The standard deviations are smaller when $r = 0.2$ which is reasonable since 80% of data are clean and only 50% of data are clean when $r = 0.5$.

In Figure 12, we show the relative errors in L^∞ -norm obtained by Algorithm 2 with $r = 0.2, 0.5$ on the left and right panel respectively. Under both settings, the

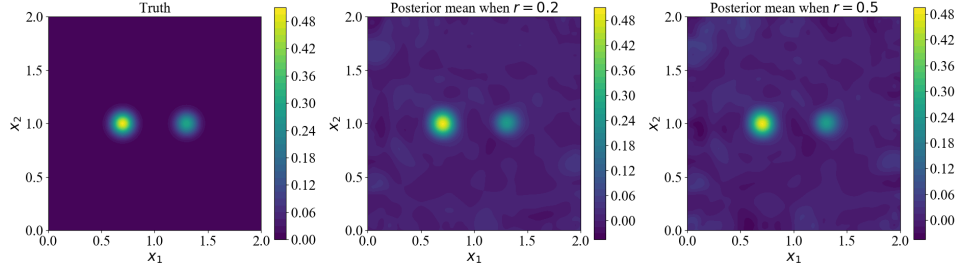


FIGURE 10. Left panel: The true source function; Middle panel: The posterior mean estimate provided by Algorithm 2 from noisy data with $r = 0.2$ (20% of data are polluted); Right panel: The posterior mean estimate provided by Algorithm 2 from noisy data with $r = 0.5$ (50% of data are polluted).

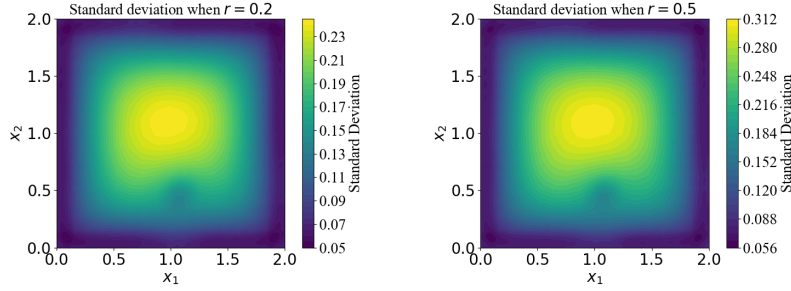


FIGURE 11. Standard deviation of the numerical solution obtained by Algorithm 3 combined with Algorithm 2. Left panel: Estimated standard deviation when $r = 0.2$ (20% of data are polluted); Right panel: Estimated standard deviation when $r = 0.5$ (50% of data are polluted).

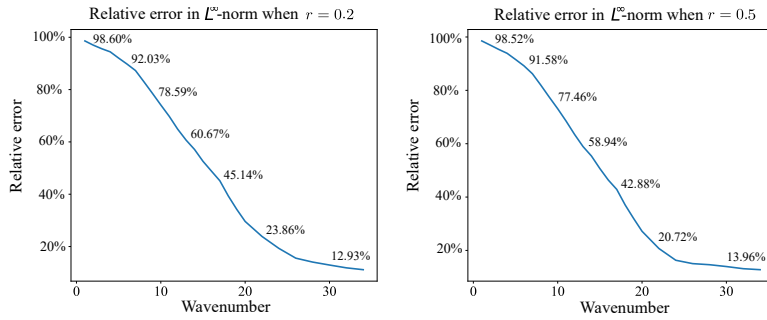


FIGURE 12. Relative errors in L^∞ -norm of Algorithm 3 combined with Algorithm 2. Left panel: Relative errors for $r = 0.2$; Right panel: Relative errors for $r = 0.5$.

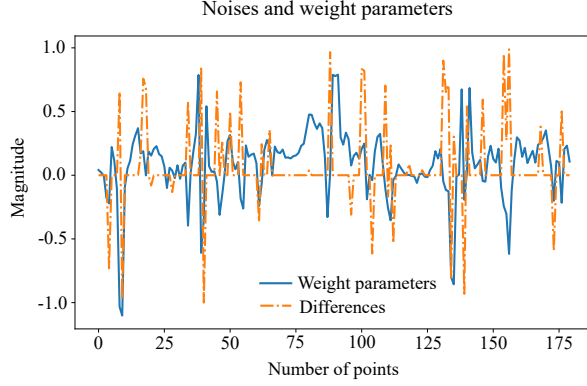


FIGURE 13. Comparison between rescaled weight parameters and rescaled noisy parts of data (Wavenumber = 34) when $r = 0.2$. The blue solid line represents the rescaled weight parameters; The dashed orange line represents the rescaled differences between clean and noisy data.

relative errors of the posterior mean estimates decrease quickly. Finally, in Figure 13, we present the rescaled weight parameters and rescaled differences between clean and noisy data when $r = 0.2$. Clearly, the weight parameters take small values at the points where data are contaminated by impulsive noises, which reflects why Algorithm 2 is robust with respect to outliers.

5. CONCLUSION

In this paper, we generalize the finite-dimensional mean-field approximate based variational Bayes' method (VBM) to infinite-dimensional space, which provides mathematical foundations for applying VBM to inverse problems of PDEs. General theory for existence of minimizers is established, and, by introducing the concept of reference probability measure, mean-field approximate theory has been constructed for functions. Then, the established general theory has been applied to abstract linear inverse problems with Gaussian and Laplace noise assumptions. Finally, numerical examples for inverse source problems of Helmholtz equations have been investigated in detail, which illustrate the effectiveness of the proposed theory and algorithms.

There are numerous interesting problems worth to be investigated, e.g., give some principles for choosing the initial values, employ other distance functions such as Stein discrepancy, use mixture of Gaussian measure to nonlinear problems.

6. APPENDIX

In this section, we collect all the proof details of the lemmas and theorems presented in this paper.

Proof of Lemma 2.2

Proof. Let $\{\nu_n\}_{n=1}^\infty = \{\prod_{i=1}^M \nu_n^i\}_{n=1}^\infty$ be a sequence of measures in \mathcal{C} that converges weakly to a probability measure ν_* . We want to show that $\nu_* \in \mathcal{C}$. Define

$$(6.1) \quad \nu_*^i := \int_{\prod_{j \neq i} \mathcal{H}_j} d\nu_*, \quad \text{for } i = 1, 2, \dots, M.$$

Obviously, each ν_*^i is a probability measure. Let f_i be some bounded continuous function defined on \mathcal{H}_i with $i = 1, 2, \dots, M$. By the definition of weak convergence, we obtain

$$(6.2) \quad \int_{\prod_{j=1}^M \mathcal{H}_j} f_i d\nu_n \rightarrow \int_{\mathcal{H}_i} f_i d\nu_*^i, \quad \text{as } n \rightarrow \infty.$$

Noticing the left hand side of (6.2) is equal to

$$(6.3) \quad \int_{\mathcal{H}_i} f_i d\nu_n^i,$$

we finally obtain that each ν_n^i converges weakly to ν_*^i . Hence, we have ν_*^i belongs to \mathcal{A}_i . Let f be a bounded continuous function defined on $\prod_{j=1}^M \mathcal{H}_j$, then it is a bounded continuous function for each variable. By the definition of weak convergence, we find that

$$(6.4) \quad \int_{\prod_{j=1}^M \mathcal{H}_j} f d\nu_n \rightarrow \int_{\prod_{j=1}^M \mathcal{H}_j} f d\nu_*,$$

and

$$(6.5) \quad \int_{\prod_{j=1}^M \mathcal{H}_j} f d\nu_n = \int_{\prod_{j=1}^M \mathcal{H}_j} f d\nu_n^1 \cdots d\nu_n^M \rightarrow \int_{\prod_{j=1}^M \mathcal{H}_j} f d\nu_*^1 \cdots d\nu_*^M,$$

when $n \rightarrow \infty$. Relying on the arbitrariness of f , we conclude that $\nu_* = \prod_{j=1}^M \nu_*^j$ which completes the proof. \square

Proof of Theorem 2.5

Proof. From the proof of Lemma 2.2, we know that ν_n^j converges weakly to ν_*^j for every $j = 1, 2, \dots, M$. According to $\nu_n^j \ll \nu^j$ for $j = 1, 2, \dots, M$, we have

$$(6.6) \quad \begin{aligned} D_{\text{KL}}(\nu_n || \nu_*) &= \int \frac{d\nu_n}{d\nu_*} \log \left(\frac{d\nu_n}{d\nu_*} \right) d\nu_* = \sum_{j=1}^M \int \log \left(\frac{d\nu_n^j}{d\nu_*^j} \right) d\nu_n^j \\ &= \sum_{j=1}^M D_{\text{KL}}(\nu_n^j || \nu_*^j). \end{aligned}$$

Using Lemma 2.4 proved in [35] and Lemma 22 shown in [16], we obtain ν_n converges to ν_* in total-variation norm, which combined with the above equality (6.6) complete the proof. \square

Proof of Lemma 2.8

Proof. For a fixed j , let $B \in \mathcal{M}(\mathcal{H}_j)$, and $\nu_n^j \in \mathcal{A}_j$ be a sequence converges weakly to ν_*^j and

$$(6.7) \quad \frac{d\nu_n^j}{d\nu_*^j} = \frac{1}{Z_{nr}^j} \exp(-\Phi_j^{nr}(x_j)).$$

Firstly, assuming $\mu_r^j(B) = 0$, then we have

$$(6.8) \quad \nu_n^j(B) = \int_B \frac{1}{Z_{nr}^j} \exp(-\Phi_j^{nr}(x_j)) \mu_r^j(dx_j) \leq \frac{e^N}{Z_{nr}^j} \mu_r^j(B) = 0.$$

Define

$$(6.9) \quad B_m = \{x \in B \mid \text{dist}(x, B^c) \geq 1/m\},$$

and let $f_m > 0$ be a positive continuous function satisfy

$$f_m(x) = \begin{cases} 1, & x \in B_m, \\ 0, & x \in B^c. \end{cases}$$

Then, we have

$$(6.10) \quad \nu_*^j(B_m) \leq \int_{\mathcal{H}_j} f_m d\nu_*^j = \lim_{n \rightarrow \infty} \int_{\mathcal{H}_j} f_m d\nu_n^j \leq \lim_{n \rightarrow \infty} \nu_n^j(B) = 0,$$

and

$$(6.11) \quad \nu_*^j(B) = \sup_m \nu_*^j(B_m) = 0,$$

where we used inner regular property of finite Borel measures. Hence, there exist a constant and a continuous function denoted as Z_r^j and $\Phi_j^r(\cdot)$ such that

$$(6.12) \quad \frac{d\nu_*^j}{d\mu_r^j}(x_j) = \frac{1}{Z_r^j} \exp(-\Phi_j^r(x_j)).$$

For completing the proof, we should verify the almost surely positiveness of the right-hand side of the above equality. Assume $\frac{1}{Z_r^j} \exp(-\Phi_j^r(x_j)) = 0$ on a set $B \subset \mathcal{H}_j$ with $\mu_r^j(B) > 0$. If $B \subset \mathcal{H}_j \setminus \sup_{N_b} T_{N_b}^j$, then $\mu_r^j(B) = 0$ by our assumption. Hence, $B \cap \sup_{N_b} T_{N_b}^j$ is not empty, and there exists a constant \tilde{N}_b such that for all $N_b \geq \tilde{N}_b$, $B \cap T_{N_b}^j$ is not empty. Denote $B_{N_b} = B \cap T_{N_b}^j$, then for N_b large enough, we have $\mu_r^j(B_{N_b}) \geq \frac{1}{2} \mu_r^j(B)$. Let

$$B_{N_b}^m = \{x \in B_{N_b} \mid \text{dist}(x, B_{N_b}^c) \geq 1/m\},$$

and define a function g_m similar to f_m with B_m replaced by $B_{N_b}^m$. Because $\mu_r^j(B_{N_b}) = \sup_m \mu_r^j(B_{N_b}^m)$, for a large enough m , we find that

$$\mu_r^j(B_{N_b}^m) \geq \frac{1}{2} \mu_r^j(B_{N_b}) \geq \frac{1}{4} \mu_r^j(B) > 0.$$

By the definition of weak convergence, we have

$$(6.13) \quad \lim_{n \rightarrow \infty} \int_{\mathcal{H}_j} g_m(x) \frac{1}{Z_{nr}^j} \exp(-\Phi_j^{nr}(x)) d\mu_r^j = \int_{\mathcal{H}_j} g_m(x) \frac{1}{Z_r^j} \exp(-\Phi_j^r(x)) d\mu_r^j.$$

The right hand side is equal to 0, however, for large enough m , the left hand side is positive and the lower bound is

$$(6.14) \quad \frac{1}{4} \exp(-C_{N_b}) \mu_r^j(B).$$

This is a contradiction, hence, the proof is completed. \square

Proof of Theorem 2.9

Proof. The existence are ensured by Lemma 2.8 and Theorem 2.3. In the following, we focus on the deduction of formula (2.19). Inserting the prior probability measure into the Kullback-Leibler divergence between ν and μ , we find that

$$\begin{aligned} D_{\text{KL}}(\nu||\mu) &= \int_{\mathcal{H}} \log \left(\frac{d\nu}{d\mu_r} \right) - \log \left(\frac{d\mu_0}{d\mu_r} \right) - \log \left(\frac{d\mu}{d\mu_0} \right) d\nu \\ &= \int_{\mathcal{H}} \left(- \sum_{i=1}^M \Phi_i^r(x_i) + \Phi^0(x) + \Phi(x) + \log Z_\mu + \log Z_0 \right) d\nu + \text{Const} \\ &= \int_{\mathcal{H}_i} \left[\int_{\prod_{j \neq i} \mathcal{H}_j} \left(\Phi^0(x) + \Phi(x) + \log Z_\mu + \log Z_0 \right) \prod_{j \neq i} \nu^j(dx_j) \right] \nu^i(dx_i) \\ &\quad - \int_{\mathcal{H}_i} \Phi_i^r(x_i) \nu^i(dx_i) + \text{terms not related to } \Phi_i(x_i). \end{aligned}$$

For $i = 1, 2, \dots, M$, let $\tilde{\nu}^i$ be a probability measure defined as follow

$$(6.15) \quad \frac{d\tilde{\nu}^i}{d\mu_r^i} \propto \exp \left(- \int_{\prod_{j \neq i} \mathcal{H}_j} \left(\Phi^0(x) + \Phi(x) + \log Z_\mu + \log Z_0 \right) \prod_{j \neq i} \nu^j(dx_j) \right).$$

Hence, we easily obtain

$$\begin{aligned} (6.16) \quad D_{\text{KL}}(\nu||\mu) &= - \int_{\mathcal{H}_i} \log \left(\frac{d\tilde{\nu}^i}{d\mu_r^i} \right) d\nu^i + \int_{\mathcal{H}_i} \log \left(\frac{d\nu^i}{d\mu_r^i} \right) d\nu^i + \text{Const} \\ &= D_{\text{KL}}(\nu^i||\tilde{\nu}^i) + \text{terms not related to } \nu^i. \end{aligned}$$

Obviously, in order to attain the infimum of the Kullback-Leibler divergence, we should take $\nu^i = \tilde{\nu}^i$. Comparing formula (6.15) with definition (2.14), we notice that the condition $\nu^i = \tilde{\nu}^i$ implies the following equality

$$\Phi_i^r(x_i) = \int_{\prod_{j \neq i} \mathcal{H}_j} \left(\Phi^0(x) + \Phi(x) + \log Z_\mu + \log Z_0 \right) \prod_{j \neq i} \nu^j(dx_j) + \text{Const},$$

which completes our proof. \square

ACKNOWLEDGMENTS

This work was partially supported by the NSFC under the grants Nos. 11871392, 11501439, 11771347, 11131006 and 41390450. and partially supported by the Major projects of the NSFC under grant Nos. 41390450 and 41390454, and partially supported by the postdoctoral science foundation project of China under grant no. 2017T100733.

REFERENCES

- [1] S. Agapiou, M. Burger, M. Dashti, and T. Helin. Sparsity-promoting and edge-preserving maximum a posteriori estimators in non-parametric Bayesian inverse problems. *Inverse Problems*, 34(4):045002, 2018.
- [2] D. F. Andrews and C. L. Mallows. Scale mixtures of normal distributions. *Journal of the Royal Statistical Society: Series B (Methodological)*, 36(1):99–102, 1974.
- [3] G. Bao, S. N. Chow, P. Li, and H. Zhou. Numerical solution of an inverse medium scattering problem with a stochastic source. *Inverse Problems*, 26:074014, 2010.
- [4] G. Bao, P. Li, J. Lin, and F. Triki. Inverse scattering problems with multi-frequencies. *Inverse Problems*, 31:093001, 2015.
- [5] G. Bao, S. Lu, W. Rundell, and B. Xu. A recursive algorithm for multi-frequency acoustic inverse source problems. *SIAM Journal on Numerical Analysis*, 53:1608–1628, 2015.

- [6] C. M. Bishop. *Pattern Recognition and Machine Learning*. Springer-Verlag, New York, NY, USA, 2006.
- [7] T. Bui-Thanh, O. Ghattas, J. Martin, and G. Stadler. A computational framework for infinite-dimensional Bayesian inverse problems part i: The linearized case, with application to global seismic inversion. *SIAM Journal on Scientific Computing*, 35(6):A2494–A2523, 2013.
- [8] M. Burger and F. Lucka. Maximum a posteriori estimates in linear inverse problems with log-concave priors are proper Bayes estimators. *Inverse Problems*, 30(11):114004, 2014.
- [9] D. Calvetti, M. Dunlop, E. Somersalo, and A. M. Stuart. Iterative updating of model error for Bayesian inversion. *Inverse Problems*, 34:025008, 2018.
- [10] D. Calvetti, O. Ernst, and E. Somersalo. Dynamic updating of numerical model discrepancy using sequential sampling. *Inverse Problems*, 30:114019, 2014.
- [11] M. A. Chappell, A. R. Groves, B. Whitcher, and M. W. Woolrich. Variational bayesian inference for a nonlinear forward model. *IEEE Transactions on Signal Processing*, 57(1):223–236, 2009.
- [12] J. Cheng, V. Isakov, and S. Lu. Increasing stability in the inverse source problem with many frequencies. *Journal of Differential Equations*, 260:4786–4804, 2016.
- [13] S. L. Cotter, G. O. Roberts, A. M. Stuart, and D. White. MCMC methods for functions: modifying old algorithms to make them faster. *Statistical Science*, 28(3):424–446, 2013.
- [14] T. Cui, K. J. H. Law, and Y. M. Marzouk. Dimension-independent likelihood-informed MCMC. *Journal of Computational Physics*, 304:109–137, 2016.
- [15] M. Dashti, K. JH Law, A. M. Stuart, and J. Voss. MAP estimators and their consistency in Bayesian nonparametric inverse problems. *Inverse Problems*, 29(9):095017, 2013.
- [16] M. Dashti and A. M. Stuart. The Bayesian approach to inverse problems. *Handbook of Uncertainty Quantification*, pages 311–428, 2017.
- [17] M. M. Dunlop and A. W. Stuart. MAP estimators for piecewise continuous inversion. *Inverse Problems*, 32(10):105003, 2016.
- [18] P. Dupuis and R. S. Ellis. *A Weak Convergence Approach to the Theory of Large Deviations*. John Wiley & Sons, New York, 1997.
- [19] Z. Feng and J. Li. An adaptive independence sampler MCMC algorithm for Bayesian inferences of functions. *SIAM Journal on Scientific Computing*, 40(3):A1310–A1321, 2018.
- [20] N. Guha, X. Wu, Y. Efendiev, B. Jin, and B. K. Mallick. A variational Bayesian approach for inverse problems with skew-t error distribution. *Journal of Computational Physics*, 301:377–393, 2015.
- [21] T. Helin and M. Burger. Maximum a posteriori probability estimates in infinite-dimensional Bayesian inverse problems. *Inverse Problems*, 31(8):085009, 2015.
- [22] V. Isakov and S. Lu. Increasing stability in the inverse source problem with attenuation and many frequencies. *SIAM, Journal on Applied Mathematics*, 78(1):1–18, 2018.
- [23] V. Isakov and S. Lu. Inverse source problems without (pseudo) convexity assumptions. *Inverse Problems & Imaging*, 12(4):955–970, 2018.
- [24] K. Ito and B. Jin. *Inverse Problems: Tikhonov Theory and Algorithms*. World Scientific, 2015.
- [25] J. Jia, B. Wu, J. Peng, and J. Gao. Recursive linearization method for inverse medium scattering problems with complex mixture Gaussian error learning. *Inverse Problems*, 2019.
- [26] B. Jin. A variational Bayesian method to inverse problems with impulsive noise. *Journal of Computational Physics*, 231:423–435, 2012.
- [27] B. Jin and J. Zou. Hierarchical Bayesian inference for ill-posed problems via variational method. *Journal of Computational Physics*, 229(19):7317–7343, 2010.
- [28] J. P. Kaipio and E. Somersalo. *Statistical and Computational Inverse Problems*. Springer Science & Business Media, Berlin, 2005.
- [29] M. Lassas and S. Siltanen. Can one use total variation prior for edge-preserving Bayesian inversion? *Inverse Problems*, 20(5):1537, 2004.
- [30] S. W. X. Lim. *Bayesian inverse problems and seismic inversion*. PhD thesis, University of Oxford, 2016.
- [31] A. Logg, K. A. Mardal, and G. N. Wells. *Automated Solution of Differential Equations by the Finite Element Method*. Springer, 2012.
- [32] Y. Ma and D. Hale. Quasi-Newton full-waveform inversion with a projected Hessian matrix. *Geophysics*, 77(5):R207–R216, 2012.

- [33] A. G. D. G. Matthews. *Scalable Gaussian process inference using variational methods*. PhD thesis, University of Cambridge, 9 2016.
- [34] F. J. Pinski, G. Simpson, A. M. Stuart, and H. Weber. Algorithms for Kullback-Leibler approximation of probability measures in infinite dimensions. *SIAM Journal on Scientific Computing*, 37(6):A2733–A2757, 2015.
- [35] F. J. Pinski, G. Simpson, A. M. Stuart, and H. Weber. Kullback-Leibler approximation for probability measures on infinite dimensional space. *SIAM Journal on Mathematical Analysis*, 47(6):4091–4122, 2015.
- [36] M. Reed and B. Simon. *Methods of Modern Mathematical Physics. I. Functional Analysis*. Academic Press, New York, 2 edition, 1975.
- [37] A. M. Stuart. Inverse problems: A Bayesian perspective. *Acta Numerica*, 19:451–559, 2010.
- [38] A. Tarantola. *Inverse Problem Theory and Methods for Model Parameter Estimation*. SIAM, 2005.
- [39] K. Yang, N. Guha, Y. Efendiev, and B. K. Mallick. Bayesian and variational Bayesian approaches for flows in heterogeneous random media. *Journal of Computational Physics*, 345:275–293, 2017.
- [40] C. Zhang, J. Butepage, H. Kjellstrom, and S. Mandt. Advances in variational inference. *IEEE Transactions on Pattern Analysis and Machine Intelligence*, pages 1–1, 2018.
- [41] Q. Zhao, D. Meng, Z. Xu, W. Zuo, and Y. Yan. l_1 -norm low-rank matrix factorization by variational Bayesian method. *IEEE Transactions on Neural Networks and Learning Systems*, 26(4):825–839, 2015.

SCHOOL OF MATHEMATICS AND STATISTICS, XI’AN JIAOTONG UNIVERSITY, XI’AN, 710049, CHINA

E-mail address: `jjx323@xjtu.edu.cn`

SCHOOL OF MATHEMATICS AND STATISTICS, XI’AN JIAOTONG UNIVERSITY, XI’AN, 710049, CHINA

E-mail address: `timmy.zhaoqian@xjtu.edu.cn`

SCHOOL OF MATHEMATICS AND STATISTICS, XI’AN JIAOTONG UNIVERSITY, XI’AN, 710049, CHINA

E-mail address: `dymeng@mail.xjtu.edu.cn`

SCHOOL OF MATHEMATICS AND STATISTICS, XI’AN JIAOTONG UNIVERSITY, XI’AN, 710049, CHINA

E-mail address: `zbxu@mail.xjtu.edu.cn`